




Skeletal muscle adaptation to muscle activity and hypoxia: Differential structural and metabolic remodelling

David Hauton¹, Roger W.P. Kissane^{2,3} , James McCullagh¹  and Stuart Egginton³ 

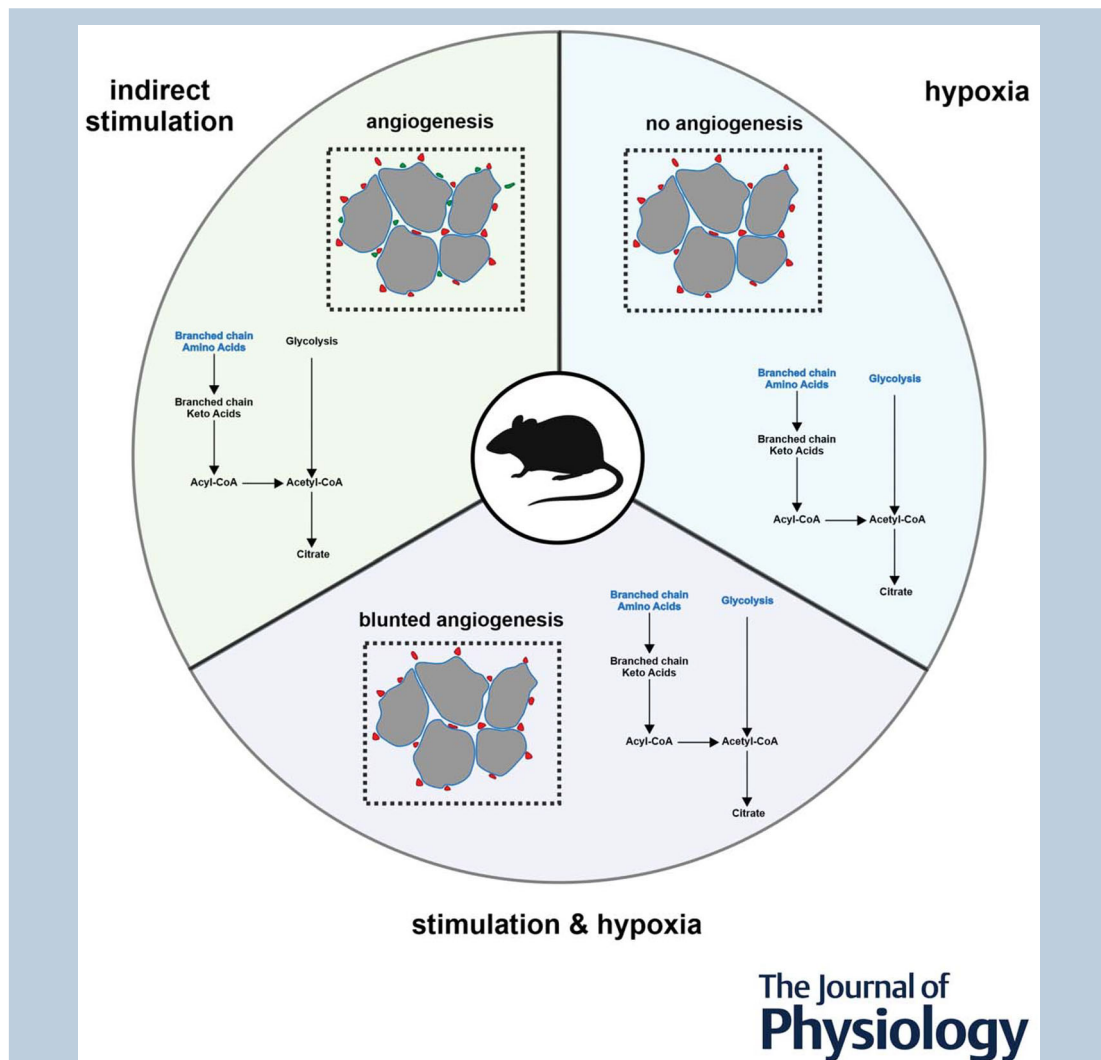
¹Department of Chemistry, University of Oxford, Oxford, UK

²Department of Musculoskeletal & Ageing Science, Faculty of Health & Life Sciences, University of Liverpool, Liverpool, UK

³School of Sport and Exercise Sciences, Faculty of Biosciences, University of Leeds, Leeds, UK

Handling Editors: Ken O'Halloran & Martino Franchi

The peer review history is available in the Supporting Information section of this article (<https://doi.org/10.1113/JP290009#support-information-section>).



Abstract figure legend There has been controversy about the structural (capillary) response of skeletal muscle to altered O₂ status, involving decreased supply (hypoxia) or increased demand (activity). Here we demonstrate that

D. Hauton and R. W. P. Kissane contributed equally to this work.

seven days of activation of skeletal muscle by indirect electrical stimulation led to significant expansion of the capillary bed. However, a similar adaptive structural response was not observed following hypoxia. When combining indirect stimulation and hypoxia, hypoxia appears to blunt structural remodelling. Proximate metabolites of the glycolytic pathway were significantly reduced following hypoxia, but not stimulation. Together these observations suggest that mechanotransduction (via indirect stimulation) triggers structural remodelling of muscle that preserves the metabolome of muscle tissue, while chemotransduction (via hypoxia) inhibits the angiogenic response induced by stimulation, possibly because of altered glycolytic metabolism.

Abstract Delivery and utilisation of oxygen are critical determinants of skeletal muscle function, and therefore aerobic performance. Angiogenesis, the process of microvascular bed expansion, may be initiated by several tissue-level stimuli (e.g. of haemodynamic, myogenic or metabolic origin), which are typically present during dynamic exercise. Understanding the relative contribution of these distinct physiological stimuli to skeletal muscle remodelling is needed to develop effective therapeutic strategies to alleviate impaired tissue oxygen supply. In the present study, we uncoupled the predominantly mechanotransductive (i.e. elevated vascular shear stress and cyclical muscle activation) and predominantly chemotransductive (i.e. local tissue hypoxia) stimuli present during exercise by exposing C57b6 mice to either indirect muscle stimulation (10 Hz; ST) or systemic hypoxia (10% oxygen; H), for 7 days, respectively. Furthermore, we combined these stimuli (H+ST) to determine whether the effects were additive. After 7 days of intervention, the tibialis anterior muscle was sampled for histological quantification of microvascular supply and metabolomics analysis. We showed that ST promoted a significant angiogenic response within the muscle whereas H did not. Interestingly, the combined H+ST group had a blunted angiogenic response. Branch-chain amino acid levels were significantly decreased following ST, H and H+ST, consistent with an increased metabolic requirement for ATP, which represents an energy deficit. Proximate metabolites of the glycolytic pathway were significantly reduced following hypoxia, but not stimulation. Together, these observations are commensurate with mechanotransduction triggering structural remodelling of muscle that preserves the metabolome of muscle tissue, whereas chemotransduction inhibits the angiogenic response induced by ST, possibly as a consequence of altered glycolytic metabolism.

(Received 28 August 2025; accepted after revision 24 February 2026; first published online 18 March 2026)

Corresponding author S. Egginton: School of Biomedical Sciences, Faculty of Biological Sciences, University of Leeds, Leeds, LS2 9JT, UK. Email: s.egginton@leeds.ac.uk

Key points

- Angiogenesis, the process of microvascular bed expansion, may be initiated by several tissue-level stimuli (e.g. haemodynamic, myogenic or metabolic in origin), which are typically present during dynamic exercise.
- There has been controversy about the structural (capillary) response of skeletal muscle to altered O₂ status, involving decreased supply (hypoxia) or increased demand (activity).
- Here, we demonstrate that 7 days of activation of skeletal muscle by indirect electrical stimulation led to significant expansion of the capillary bed. However, a similar adaptive structural response was not observed following hypoxia. When combining indirect stimulation and hypoxia, hypoxia appears to blunt structural remodelling.
- Proximate metabolites of the glycolytic pathway were significantly reduced following hypoxia, but not stimulation.
- Together, these observations suggest that mechanotransduction (via indirect stimulation) triggers structural remodelling of muscle that preserves the metabolome of muscle tissue, whereas chemotransduction (via hypoxia) inhibits the angiogenic response induced by stimulation, possibly because of altered glycolytic metabolism.

Introduction

Skeletal muscle is highly plastic, able to differentially modulate the distribution of capillaries (oxygen supply network) and mitochondrial composition (sites of oxygen demand) to accommodate function during ontogenetic growth (Young & Egginton, 2009), physiological exercise (Liu et al., 2022) and pathophysiological remodelling (Warren et al., 2020). The ability of skeletal muscle to sustain function is highly dependent on a complex interplay between supply and demand for O₂ (Kissane et al., 2021; Tickle et al., 2020). Remodelling of microvascular supply vessels and muscle metabolome exhibits distinct temporal responses, which depend on the underlying drivers (e.g. mechanotransductive vs. chemotransductive stimuli) (Egginton, 2009; Kissane & Egginton, 2019; Kissane et al., 2023).

Exercise is one of the most common physiological remodelling stimuli used to expand the capillary bed (Liu et al., 2022) and differentially modulate muscle metabolism (Smith et al., 2023). Yet, the relative contribution of these stimuli to the adaptive remodelling process is difficult to separate. During exercise, skeletal muscle is subjected to a range of mechanotransductive signals from elevated vascular shear stress and transmural pressure, as well as cyclical muscle stretch (Egginton, 2009). Individually, these signals are potent angiogenic stimuli (Williams, Weichert, et al., 2006; Williams, Cartland, Hussain, et al., 2006) and are able to enhance muscle fatigue resistance (Kissane et al., 2020; Scott et al., 1985; Tickle et al., 2020). However, little is known of the holistic remodelling of the microvascular and metabolic systems in response to elevated mechanotransduction. Indirect electrical stimulation (ST) of muscle has been utilised to differentially regulate the levels of hyperaemia and muscle force recruitment (Kissane et al., 2023) and provides a unique opportunity to explore the dynamic remodelling of both structural and metabolic characteristics. This approach increases oxygen demand and is expected to be consistent with estimates of intracellular P_{O₂} during exercise (Poole & Musch, 2023) at the same time as avoiding volitional input or imposed stress.

Classic studies highlighted that chronic ST increased activity of muscle fibre succinate dehydrogenase activity

(Pette & Tyler, 1983), as well as citrate synthase and malate dehydrogenase (Buechegger et al., 1984), implying that enhanced muscle fatigue resistance is partly a result of increased oxidative activity. Coupled with decreased lactate dehydrogenase activity (Buechegger et al., 1984), this suggests a metabolic realignment from glycolytic capacity towards a more oxidative phenotype. Furthermore, chronic ST of skeletal muscle not only led to hypertrophy of type I and type II fibres, but also a transition from fast-twitch to slow-twitch (oxidative) fibres (Gondin et al., 2011). More recently, we demonstrated that graded ST of skeletal muscle in the rat resulted in a graded structural response, characterised by higher capillary density and lower calculated regions of muscle hypoxia (Kissane et al., 2023). However, the metabolic response was not graded, suggesting an incomplete transition to a new metabolic equilibrium.

Hypoxia is potent modulatory signal across both central and peripheral systems (Deveci et al., 2001; Doody et al., 2024; Nagahisa & Miyata, 2018; Warren et al., 2020) and the consequence of the pattern (continuous vs. intermittent) and duration (acute vs. chronic) on adaptive remodelling is a continuing topic of interest (Lemieux & Birot, 2021). Chronic hypoxia exposure (over 3 weeks) is able to significantly enhance microvascular supply in slow phenotype muscles (e.g. soleus and diaphragm), whereas no appreciable change was seen in fast phenotype muscles [e.g. extensor digitorum longus and tibialis anterior (TA)] (Deveci et al., 2001). However, a caveat must be that skeletal muscle is heterogeneous in myofibre phenotype and microvascular supply (Deveci et al., 2001; Kissane et al., 2018; Kissane et al., 2019; Olfert et al., 2016) and, upon finer scale compartmental analysis, the most glycolytic portions of the TA also showed an angiogenic expansion in response to hypoxia (Deveci et al., 2001). Metabolomic analysis has suggested that hypoxia may lead to an insulin-resistant-like phenotype within skeletal muscle (Margolis et al., 2021), associated with decreased glucose clearance and increased branch chain amino acid (BCAA) accumulation. This study utilised an acute exposure to an F_IO₂ = 0.13, similar to that encountered for chronic obstructive pulmonary disease (COPD) patients.

Accordingly, the next logical question to address is how does the combination of these two divergent signalling

David Hauton is currently lecturer in Pharmacology at the University of Bath. Working as an integrative physiologist, Dave has focused on the metabolic contribution of muscle performance using labelling studies and metabolomics. **Roger W. P. Kissane** is currently a research fellow at the University of Liverpool. This work presented here formed part of his PhD at the University of Leeds understanding the mechanisms of activity induced angiogenesis.



paradigms interact? Studies that comprehensively quantify these interactions are lacking, but necessary to understand the integrated angiogenic response and metabolic profile changes. A combination of exercise training with chronic hypoxia in rodents indicated no improvement in structural remodelling of microvascular supply (Olfert et al., 2001). Similarly, in humans, exercising in normoxia significantly increased muscle vascular endothelial growth factor (VEGF), whereas, in hypoxia, the same exercise stimulus led to a reduced VEGF response, thus blunting the angiogenic response (Richardson et al., 2000). Furthermore, combining both stimuli led to decreased blood glucose concentrations compared to hypoxia alone, implying increased glucose utilisation (Katayama et al., 2018). Yet, 4 weeks of high-intensity exercise in hypoxia increased nitric oxide (NO) bioavailability and improved vascular function (Lavier et al., 2021). Early experiments demonstrated that both ST and hypoxia led to increased glucose uptake, but the former induced a greater response and exploited a different signalling pathway, implying a potential augmentation of the metabolic contribution from glucose with combined stimuli (Friolet et al., 1994). However, acute exercise under acute hypoxia increased muscle acetyl-CoA and free carnitine, coupled with decreased esterified coenzyme A, implying utilisation of fatty acids to enhance acetyl-CoA production (Friolet et al., 1994), which in turn fuels ATP production via oxidative phosphorylation and modulates the switch between glucose and fatty acid oxidation.

Taken together, these observations imply that there are distinct structural and metabolic adaptations to both stimuli individually. What is unclear is whether these effects are synergistic and to what degree hypoxia may potentiate the acute adaptive response to indirect stimulation (Lemieux & Birot, 2021). Exploiting an integrated approach consisting of histological and metabolomic analysis for the TA muscle in mice, we determined the impact of indirect stimulation (ST; increasing oxygen consumption) and systemic hypoxia (H; reducing oxygen delivery) on structural and metabolic adaptations to individual stimuli and the combination of both stimuli. For the first time, we quantified the metabolic transition of the mouse TA in response to these stimuli using two separate metabolomic platforms to detect a range of central energy metabolites [reverse-phase liquid chromatography-mass spectrometry (LC-MS) analysis] or primary and secondary amines (reverse-phase LC-MS analysis of derivatised samples). We hypothesise that: angiogenesis may be elicited by a range of stimuli (ST, H and the combination of the two) (hypothesis 1) and (2) the metabolic profile of the skeletal muscles will differ in response to these differential stimuli (hypothesis 2).

Methods

Ethical approval

All animal work was approved by the University of Birmingham and University of Leeds Animal and Welfare Ethical Review Board and carried out in accordance with the Animals (Scientific Procedures) Act 1986 (under Home Office Project licence: 70/08674). This work conforms to the ethical requirements outlined by *The Journal of Physiology* in accordance with guidelines for animal work (Grundy, 2015; Percie du Sert et al., 2020). Twenty-six, 12-week-old male C57/B6 mice (sourced from an in-house breeding colony) were housed in groups of three or four under a 12:12 h light/dark photocycle at 21°C with *ad libitum* access to food and water. Animals were assigned to one of four groups (see Appendix, Fig. A1): control (CT, $n = 11$), 7 days of indirect stimulation (ST, $n = 9$), 7 days of 10% hypoxia (H, $n = 6$) or a combination of hypoxia and indirect stimulation (H+ST, $n = 6$). Note, the latter samples were sourced from the same animal and the mice received systemic hypoxia (i.e. both limbs, with a contralateral H response) and unilateral indirect stimulation (giving an ipsilateral H+ST response).

Surgical procedures

Animal surgery was conducted under aseptic conditions with inhalation anaesthetic (isoflurane; IsoFlo; Zoetis UK Limited, Leatherhead, UK), induction with 5% isoflurane (2 L min⁻¹ O₂ flow). Following the loss of withdrawal reflex (toe pinch) and eye blink response, the surgical plane was maintained with 2.5% (2 L min⁻¹ flow). Animals underwent indirect electrical stimulation of the hind limb ankle flexors via stimulation of the deep lateral peroneal nerve. Miniaturised, battery-powered electrical stimulators were coated with hypo-allergenic beeswax and placed in a subcutaneous pouch on the mid-thoracic region of the back (Linderman et al., 2000). The stimulator was inserted through a 2 cm incision and sutured into place. Stimulating electrodes made from polytetrafluoroethylene-coated seven-strand braided stainless steel wires (A-M Systems, Sequim, WA, USA) were tunnelled distally towards the right hind limb under the skin, and a loose wire loop was sutured into place near the hip to minimise tension in the wire during locomotion. Electrodes were passed through the vastus lateralis using a 23 g needle towards the peroneal nerve. Once in place, the covering fascia across the superficial muscles were closed with absorbable 6-0 suture (Ethicon/Johnson & Johnson Medical, New Brunswick, NJ, USA) and the skin closed with braided 4-0 silk suture (Ethicon/Johnson & Johnson Medical). Animals received

s.c. injections of analgesic (30 $\mu\text{g kg}^{-1}$ buprenorphine; Vetergesic, Ceva Animal Health Ltd, Amersham, UK) and antibiotic (2.5 mg kg^{-1} enrofloxacin; Baytril, Bayer, Reading, UK) immediately after surgery, repeated for 2 days post-surgery. The animals were given 24 h to recover before the stimulators were activated (see Appendix, Fig. A1), allowing sufficient time for surgical trauma/inflammation to subside and normal locomotion to resume. Control mice did not undergo a sham surgery, as previous experiments showed no discernible difference (Takahashi & Hood, 1993).

Stimulation protocol

Indirect electrical stimulation was delivered using a supramaximal voltage, pulse duration of 0.3 ms, and delivered at a preset stimulation frequency of 10 Hz continuously for 8 h day^{-1} , delivered for 7 days. This stimulation paradigm was selected based on previous findings that this stimulation frequency promotes the greatest active hyperaemia response at a submaximal force recruitment, leading to significantly elevated micro-vascular composition across the core and cortex of the TA (Kissane et al., 2023).

Hypoxia

We exposed mice to chronic systemic hypoxia in a purpose-built chamber with CO_2 scrubbing and humidity control. Chamber oxygen was reduced to a fraction of inspired oxygen (F_{IO_2}) of 0.10 (10% O_2) using an experimental approach previously implemented in mice (Davidsen et al., 2016). To minimise physiological stress, F_{IO_2} was lowered gradually from normoxia to 0.10 over the first week and then maintained at $F_{\text{IO}_2} = 0.10$ for a second week during which muscle stimulation was applied (see Appendix, Fig. A1).

Tissue sampling

Mice were culled by Schedule 1 methods, through concussion, followed by cervical dislocation, in line with the Animal Scientific Procedures Act (1986). Whole TA muscles were carefully dissected from the hind limb of the animal and weighed. Muscle samples were split into three equal portions with the proximal and distal portions frozen in liquid nitrogen for metabolomics analysis, while the mid portions were snap frozen in liquid nitrogen-cooled isopentane for histological sampling. All tissue was stored at -80°C until further use.

Histological analysis

Serial cryostat (-20°C) cross-sections (10 μm) were attached to polysine adhesion slides (VWR International,

Radnor, PA, USA), then fixed with 2% paraformaldehyde for 2 min. Following 10 washes in phosphate-buffered saline (PBS), sections were stained with *Griffonia simplicifolia* lectin-1 (Vector Laboratories, Prestwich, UK; diluted 1:200 in PBS) to identify capillaries through its affinity to proteoglycans in the glycocalyx. Slides were incubated for 1 h, then washed and mounted in VectaShield (Vector Laboratories; H-1400). Three regions of interest (0.145 mm^2) were imaged, spanning two metabolically distinct regions within the TA: the oxidative core ($\times 2$ fields) and the glycolytic cortex ($\times 2$ fields). Capillary-to-fibre ratio (C:F), capillary density (CD, mm^{-2}) and average fibre cross-sectional area (FCSA, μm^2) were derived from histological cross-sections. These commonly used global indices describe gross changes in capillary supply, but lack resolution for local spatial distribution of supply (Egginton, 1990; Kissane et al., 2021). Therefore, we present further local capillary indices of tissue supply area [capillary domain area (CDA), μm^2] and heterogeneity (through the standard deviation of the log-transformed CDA; logSD).

Tissue oxygen status were modelled on the histologically derived capillary distributions using capillary domain boundaries as geometric constraints to estimate P_{O_2} using the open access 'Oxygen Transport Modeller' (Al-Shammari et al., 2019). In our model, we simulated high oxygen demand ($\sim 1\text{--}5$ mmHg) consistent with experimental estimates of intracellular P_{O_2} during exercise (Poole & Musch, 2023), supporting its physiological validity (Al-Shammari et al., 2025). The overall tissue P_{O_2} was estimated as well as the percentage of the tissue considered to be hypoxic, which we represented by tissue $P_{\text{O}_2} < 0.5$ mmHg (Al-Shammari et al., 2019).

One potential limitation of this approach is tissue-wide coverage of metabolomics analysis, whereas the histological analysis possessed more regional focus to highlight any differential effects due to inherent fibre-specific metabolic profile. Subdivision of muscle samples to discretely analyse the metabolome of each histological sampling region yielded insufficient tissue to perform parallel analyses; therefore, we also provide histological analysis incorporating data from all regions of the muscle to facilitate comparison with the metabolomics data.

Metabolomic analysis

Reversed phase LC-MS (underivatized). Reversed-phase analysis of underivatized metabolite extracts was performed using an Ultimate 3000 UHPLC system (Thermo Fisher Scientific, Waltham, MA, USA) with a gradient elution program coupled directly to a Q-Exactive HF Hybrid Quadrupole-Orbitrap mass spectrometer (Thermo Fisher Scientific). A 5 μL partial loop injection

was used for all analyses with pre- and postinjection wash program. A CORTECS UPLC T3 1.6 μm (2.1×100 mm) column (Waters, Milford, MA, USA) was used with a flow rate of 0.4 mL min^{-1} . The total run time was 18 min. The mobile phase A comprised Milli-Q water (Merck Millipore, Burlington, MA, USA) with 0.1% formic acid and the mobile phase B was 100% methanol with 0.1% formic acid. The gradient elution program was as follows: 0 min, 5%B; 4 min, 50%B; 12 min, 99%B; 15 min, 99%B; 15.1 min, 5%B; 18 min, 5%B. The column temperature was maintained at 40°C throughout the experiment. MS analysis was performed in positive and negative ion mode separately using the scan range m/z 60–900 with the resolution set to 70,000. The tune file source parameters were set as follows: sheath gas flow 60 mL min^{-1} ; auxiliary gas flow 20 mL min^{-1} ; spray voltage 3.6 V; capillary temperature 320°C ; S-lens RF value 70; heater temperature 350°C . Full MS settings were AGC target 5×10^6 ions and the maximum IT value was 120 ms. Full scan data were acquired in continuum mode. A data-directed tandem MS method was utilised (ddMS²) with no inclusion list. The orbitrap detector and HCD setting for ddMS² were as follows: microscans 2, resolution 17,500, AGC target 5×10^4 ions, maximum IT 80 ms, loop count 10 and NCE 35.

Reversed phase LC-MS (derivatised). The LC-MS method used a sample derivatisation protocol to label 1° and 2° amines, followed by analysis based on a modified version of the Waters AccQ-Tag method (Salazar et al., 2012). Reversed-phase LC-MS analysis of derivatised samples was also performed using the Ultimate 3000 UHPLC system (Thermo Fisher Scientific) coupled directly to a Q-Exactive HF Hybrid Quadrupole-Orbitrap mass spectrometer. A $5 \mu\text{L}$ partial loop injection was used for all analyses with pre and post injection wash program. An AccQ-Tag column (2.1×100 mm) (Waters) was used with a flow rate of 0.5 mL min^{-1} . The total run time was 9.5 min. Mobile phase A and B comprised commercially available AccQ-Tag reagents prepared as recommended by Waters. The gradient elution program was modified from the published AccQ-Tag method as follows: 0 min, 0.1%B; 0.54 min, 9.1%B; 5.74 min, 21.2%B; 7.74 min, 59.6%B; 8.04 min, 90%B; 8.05 min, 90%B; 8.64 min, 0%B; 9.5 min, 0.1%B. The column temperature was kept at 40°C throughout the experiment. Mass spectrometry analysis was performed in positive ion mode separately using the scan range m/z 70–1050 with the resolution set to 70,000. The tune file source parameters were set as follows: sheath gas flow 60 mL min^{-1} ; auxiliary gas flow 20 mL min^{-1} ; spray voltage 3.6 V; capillary temperature 320°C ; S-lens RF value 70; heater temperature 350°C . Full MS settings were AGC target 3×10^6 ions and the maximum IT value was 200 ms. Full scan data were acquired in continuum mode.

Data processing

Data processing was performed according to our previously published metabolomics protocols (Walsby-Tickle et al., 2020; Williams et al., 2025). Briefly, metabolites were identified with reference to an in-house database created from authenticated standards. Pure compounds were purchased from chemical suppliers (e.g. Sigma–Aldrich, Poole UK; Tocris, Bristol, UK; Tokyo Chemicals Industry, Oxford, UK). These standards were then diluted in solvent (80% methanol) and separated chromatographically by different methods. Each compound was then examined using a Q Exactive Mass Spectrometer (Thermo Fisher Scientific). Each authenticated standard was identified by collection of discrete data: this included chromatographic retention time, accurate mass (four decimal places) and compound fragmentation, thus allowing identification of isomers with reference to differing fragmentation and retention characteristics.

Raw data files were processed using ProgenesisQI for small molecules (Waters). This process included alignment of retention times, picking by identification of natural abundance isotope peaks, characterising multiple adducts forms and identification of metabolites using our in-house database. Retention times, accurate mass values, relative isotope abundances and fragmentation patterns were compared between authentic standards and the samples measured. Identifications were accepted only when the following criteria were met: <5 ppm differences between measured and theoretical mass (based on chemical formula), <30 s differences between authenticated standard and analyte retention times, and isotope peak abundance measurements for analytes were $>90\%$ matched to the theoretical value generated from the chemical formula. Where measured, fragmentation patterns were matched to least the base peak and two additional peak matches in the MS/MS spectrum to within 12 ppm.

Statistical analysis

Histological (C:F, CD, FCSA, CDA, logSD, P_{O_2} and %hypoxia) and metabolomic data (fold-change; ratio of metabolite concentration relative to the average CT concentration) were analysed using a linear mixed model (LMM) split-plot design, with individual animal ID included as a random intercept. Data were processed in R, version 4.2.1 (R Foundation, Vienna, Austria) with group effects evaluated using type III *F* tests with Satterthwaite-adjusted denominator degrees of freedom (via the lmerTest package). *Post hoc* pairwise comparisons between levels were performed using estimated marginal means (*emmeans*), with Benjamini–Hochberg correction applied to control the false discovery rate. Principal component analysis and

partial least-squares discrimination analysis (PLS-DA) were also used to analyse the patterns in metabolomic profiles among treatments. All data are presented as the mean \pm SD. $P < 0.05$ was considered statistically significant.

Results

Histological analysis

The TA is a highly compartmentalised muscle homologous across mammals from mice, rats and humans.

This muscle generally presents with a highly oxidative core (posterior compartment) (Fig. 1A) and a highly glycolytic cortex (anterior compartment) (Fig. 2A) (Deveci et al., 2002; Kissane et al., 2023). We determined the structural remodelling induced across these two distinct compartments. Briefly, indirect stimulation presents a greater stimulus for microvascular remodelling across the mouse TA (Figs 1 and 2) than hypoxia, which induced no structural adaptations at this acute time point. The addition of hypoxia to stimulation (H+ST group) appears to blunt some structural remodelling seen in the indirect ST only group (Figs 1 and 2).

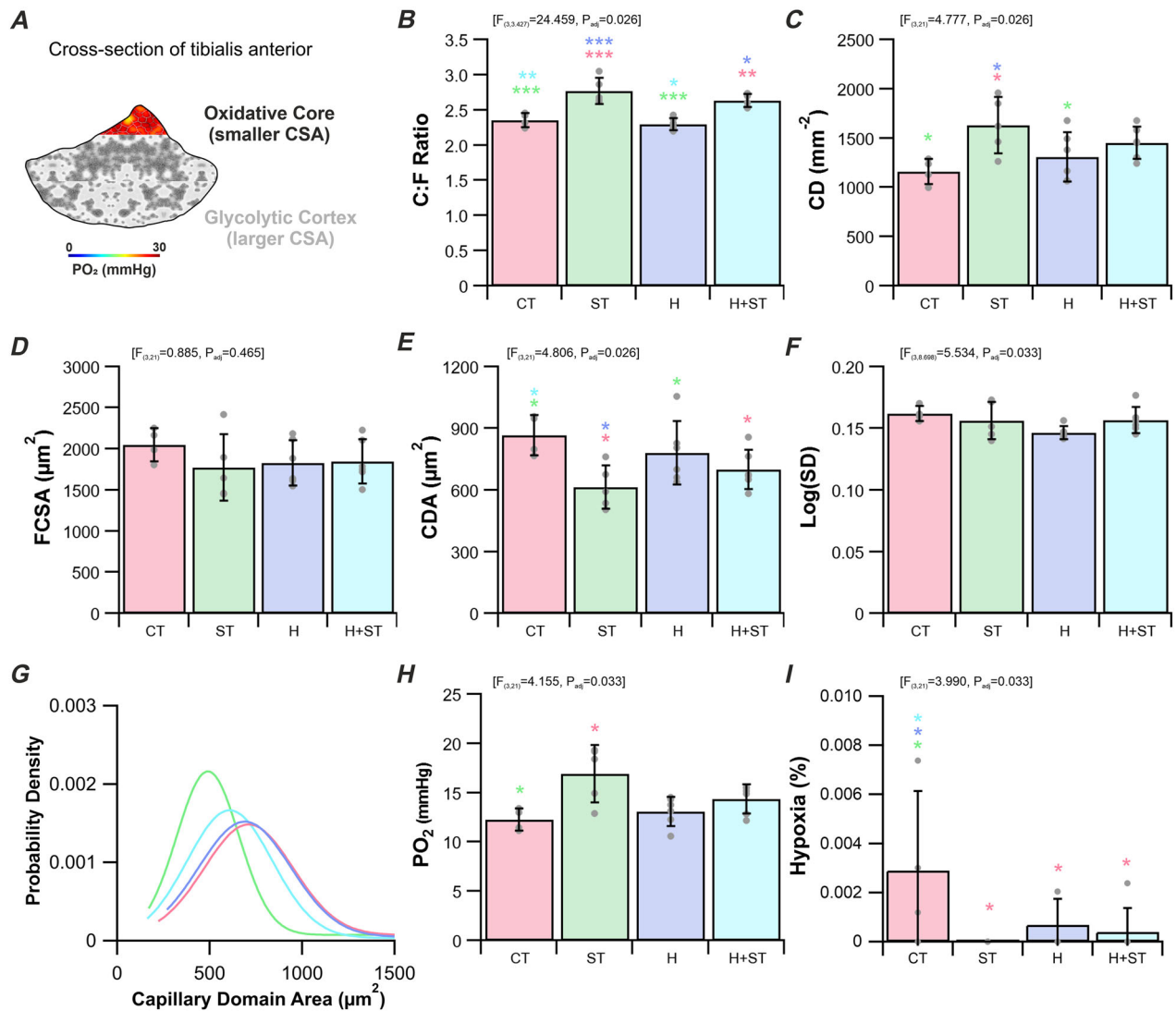


Figure 1. Angiogenic response of the mouse tibialis anterior core region

The posterior compartment of the mouse tibialis anterior contains smaller and more oxidative fibres (A). Changes in capillary-to-fibre ratio (B), capillary density (C), fibre cross-sectional area (D), capillary domain area (E) and standard deviation of the logged capillary domain area (F) and (G). Model estimates of tissue P_{O_2} (H) and hypoxia (I) for the core region of the tibialis anterior when simulated at high oxygen consumption rates (Al-Shammari et al., 2019). Data are presented as the mean \pm SD, * $P \leq 0.05$, ** $P \leq 0.01$, *** $P \leq 0.001$, colour-coded to show groups compared. Control (CT, $n = 4$), indirect stimulation (ST, $n = 5$), hypoxia (H, $n = 6$) and combination indirect stimulation and hypoxia (H+ST, $n = 6$).

Tibialis anterior (oxidative core)

Significant changes to the number of capillaries (C:F, LMM $F_{3,3.43} = 24.459$, $P_{\text{adj}} = 0.026$) (Fig. 1B) and density of capillaries (CD, LMM $F_{3,21} = 4.777$, $P_{\text{adj}} = 0.026$) (Fig. 1C) manifested after ST, with concomitant improvement in tissue oxygen status. These global changes in microvascular supply occurred independent of changes in FCSA (LMM $F_{3,21} = 0.885$, $P_{\text{adj}} = 0.465$) (Fig. 1D). Specifically, indirect stimulation significantly increased C:F compared to control levels (2.77 ± 0.18 vs. 2.36 ± 0.10 , $P < 0.001$) (Fig. 1B), and in combination with hypoxia (H+ST, 2.64 ± 0.09 , $P = 0.002$) (Fig. 1B).

Significant changes were seen in some local capillary metrics, mainly CDA (LMM $F_{3,21} = 4.806$, $P_{\text{adj}} = 0.026$) (Fig. 1E), modelled estimates of tissue P_{O_2} (LMM $F_{3,21} = 4.155$, $P_{\text{adj}} = 0.033$) (Fig. 1H) and modelled estimates of tissue hypoxia (LMM $F_{3,21} = 3.990$, $P_{\text{adj}} = 0.033$) (Fig. 1I). Indirect stimulation significantly lowered CDA compared to control (613 ± 105 vs. $867 \pm 99 \mu\text{m}^2$, $P = 0.0115$) (Fig. 1E), resulting in a leftward shift in the CDA distribution (Fig. 1F), a significant increase in modelled tissue P_{O_2} (16.9 ± 2.8 vs. 14.9 ± 2.2 mmHg, $P = 0.0158$) (Fig. 1H) and a significant decrease in the estimated area of tissue considered to be hypoxic (0.003 ± 0.003 vs. 0 ± 0 mmHg, $P = 0.0231$) (Fig. 1I).

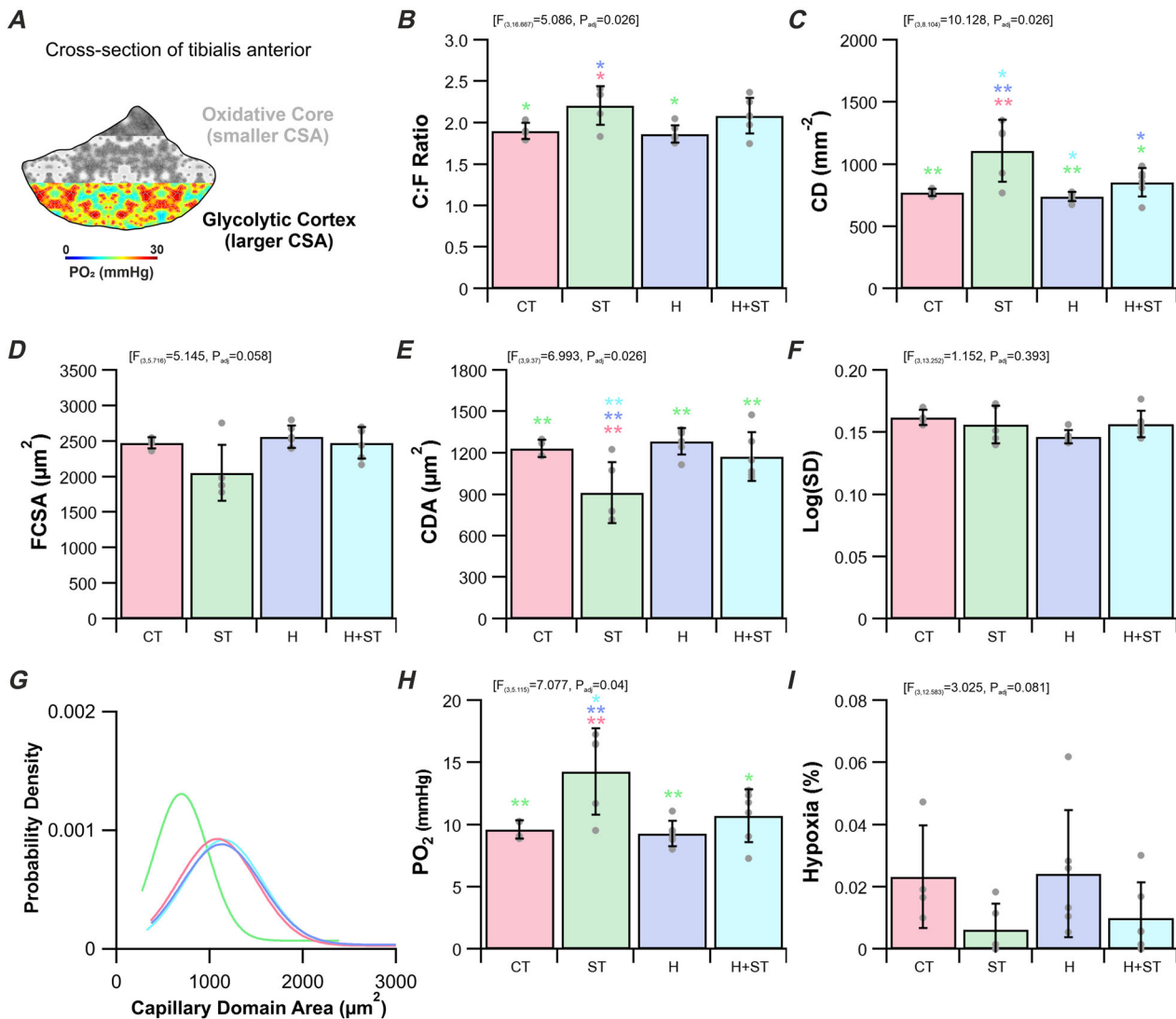


Figure 2. Angiogenic response of the mouse tibialis anterior cortex region

The anterior compartment of the mouse tibialis anterior contains larger and more glycolytic fibres (A). Changes in capillary-to-fibre ratio (B), capillary density (C), fibre cross-sectional area (D), capillary domain area (E) and standard deviation of the logged capillary domain area (F) and (G). Model estimates of tissue P_{O_2} (H) and hypoxia (I) for the cortex region of the tibialis anterior when simulated at high oxygen consumption rates (Al-Shammari et al., 2019). Data are presented as the mean \pm SD, * $P < 0.05$, ** $P < 0.01$, *** $P < 0.001$. Control (CT, $n = 4$), indirect stimulation (ST, $n = 5$), hypoxia (H, $n = 6$) and combination indirect stimulation and hypoxia (H+ST, $n = 6$).

Tibialis anterior (glycolytic cortex)

Dynamic changes to the global supply of capillaries; C:F (LMM $F_{3,16.667} = 5.086$, $P_{\text{adj}} = 0.026$) (Fig. 2B) and CD (LMM $F_{3,8.104} = 10.128$, $P_{\text{adj}} = 0.026$) (Fig. 2C) were observed alongside no statistically significant change in FCSA (LMM $F_{3,5.716} = 5.145$, $P_{\text{adj}} = 0.058$) (Fig. 2D). Here, a significant increase in CD was evident following indirect stimulation compared to control (1110 ± 248 vs. 774 ± 27 mm², $P = 0.006$) (Fig. 2C) through a significant increase in C:F (2.21 ± 0.24 vs. 1.90 ± 0.10 , $P = 0.032$) (Fig. 2B). Subsequently, indirect stimulation had a significantly higher CD compared to hypoxia alone (1307 ± 250 mm², $P = 0.002$) (Fig. 2C) and the combined stimuli (H+ST, 1453 ± 163 mm², $P = 0.0131$) (Fig. 2C). Changes at the local capillary supply level were also evident in the cortex of the TA, with significant group effects seen in improved CDA (LMM $F_{3,9.37} = 6.993$, $P_{\text{adj}} = 0.026$) (Fig. 2E and G) and modelled estimates of tissue P_{O_2} (LMM $F_{3,5.115} = 7.077$, $P_{\text{adj}} = 0.04$) (Fig. 2H). Indirect stimulation induced a significantly reduced CDA compared to control (915 ± 222 vs. 1232 ± 62 μm², $P = 0.009$) (Fig. 2E and G), whereas combining hypoxia with stimulation appeared to blunt this response (H+ST, 1175 ± 177 μm², $P = 0.563$). Subsequently, tissue P_{O_2} was only significantly elevated in the stimulation group (14.3 ± 3.5 vs. 9.6 ± 0.7 mmHg, $P = 0.0055$) (Fig. 2H).

Untargeted metabolomics

Reverse phase LC-MS (underivatised) produced 15 607 ion features with 8308 ions identified as clearly defined features (CV <30%; 53.2%). Reverse phase LC-MS (derivatised), detecting primary and secondary amines, led to 3682 ion-features with 1808 well-characterised ions (CV <30%, 49.1%). Untargeted analysis of ion-features identified using underivatised and derivatised reverse phase LC-MS (Fig. 3A and B) indicated overlap between all groups, indicating that metabolic perturbation induced by indirect stimulation, hypoxia or a combination of the two, share significant overlap in ion-features produced. PLS-DA for reverse phase LC-MS analysis indicated that modelled data correlated strongly with measured data for the different experimental groups (accuracy = 0.929; $R^2 = 0.992$; $Q^2 = 0.848$) (Fig. 3C). In addition, permutation analysis indicated a degree of 'overfitting' of data ($P = 0.073$) (Fig. 3C). PLS-DA for reverse phase LC-MS analysis (derivatised) indicated that modelled data correlated strongly with measured data for the different experimental groups (accuracy = 0.857; $R^2 = 0.999$; $Q^2 = 0.703$) (Fig. 3D) with modest separation between the experimental groups. Permutation analysis again indicated a degree of 'overfitting' ($P = 0.643$) (Fig. 3D). To identify putative metabolic pathway

perturbations, metabolite enrichment analysis was undertaken exploiting binary comparisons for ion features coupled with fold change and statistical analysis (Xia & Wishart, 2010). These ion features were matched to identified compounds in the Mummichog database based on m/z value (Li et al., 2013) and were linked with individual pathways to determine putative targets (Xia & Wishart, 2010) (Fig. 4). Binary comparisons were undertaken to determine the effect of indirect stimulation (Fig. 4A), the effect of hypoxia (Fig. 4B) and the impact of stimulation + hypoxia (Fig. 4C). Analysis of the muscle metabolome demonstrated that indirect stimulation potentially affected unsaturated fatty acid synthesis ($P = 1.47 \times 10^{-4}$), glycolysis ($P = 0.024$) and linoleic acid metabolism ($P = 0.035$). Exposure to chronic hypoxia (Fig. 4B) significantly affected metabolic pathways, including starch and sucrose metabolism ($P = 0.0032$) coupled with purine metabolism ($P = 0.041$). Combining both stimuli induced significant differences in the putative inositol phosphate pathway ($P = 8.32 \times 10^{-6}$) and led to altered glycolysis/gluconeogenesis ($P = 7.21 \times 10^{-4}$), starch and sucrose metabolism ($P = 4.27 \times 10^{-4}$) and pentose phosphate metabolism ($P = 0.0015$).

Targeted metabolomics

Muscle turnover. Mapping identified metabolites onto biochemical pathways highlighted muscle remodelling pathways, with 1-methyl histidine used as a marker for this process (Fig. 5A–G). Skeletal muscle carnosine (LMM $F_{3,28} = 25.636$, $P_{\text{adj}} < 0.001$) (Fig. 5B) and histidine (LMM $F_{3,28} = 29.238$, $P_{\text{adj}} < 0.001$) (Fig. 5F) levels were significantly modified in response to ST, H and the combined H+ST group. Carnosine levels were significantly decreased in response to stimulation (0.66 ± 0.13 FC, $P < 0.001$) (Fig. 5B), hypoxia (0.71 ± 0.11 FC, $P < 0.001$) (Fig. 5B) and combined stimuli (0.43 ± 0.17 FC, $P < 0.001$) (Fig. 5B). However, combination (H+ST) levels of carnosine were significantly lower than with individual stimuli of either indirect stimulation ($P < 0.001$) (Fig. 5B) or hypoxia ($P < 0.001$) (Fig. 5B). Comparable trends exist in histidine levels, with significant decreases in the stimulation (0.64 ± 0.13 FC, $P < 0.001$) (Fig. 5F), hypoxia (0.50 ± 0.10 FC, $P < 0.001$) (Fig. 5F) and combination (0.42 ± 0.16 FC, $P < 0.001$) (Fig. 5F) groups compared to controls. Furthermore, the combination of stimulation and hypoxia had an added response, with significantly lower levels of histidine than that of the stimulation group ($P = 0.003$) (Fig. 5F). TA muscle levels of beta-alanine (LMM $F_{3,28} = 2.197$, $P_{\text{adj}} = 0.117$) (Fig. 5C), anserine (LMM $F_{3,28} = 3.199$, $P_{\text{adj}} = 0.053$) (Fig. 5D), urocanic acid (LMM $F_{3,8.611} = 2.134$, $P_{\text{adj}} = 0.169$) (Fig. 5E) and 1-methyl histidine (LMM $F_{3,8.562} = 3.843$, $P_{\text{adj}} = 0.06$)

(Fig. 5G) were not significantly altered in response to any of the imposed interventions.

Glycolysis. All constituent metabolites within the glycolysis pathway (Fig. 6A) were significantly altered

in response to modulated oxygen status of skeletal muscle (Fig. 6B–I). Fructose 6-phosphate levels (LMM $F_{3,2,435} = 13.423$, $P_{\text{adj}} = 0.06$) (Fig. 6B) were not significantly downregulated by indirect electrical stimulation (0.85 ± 0.17 FC, $P = 0.085$), although

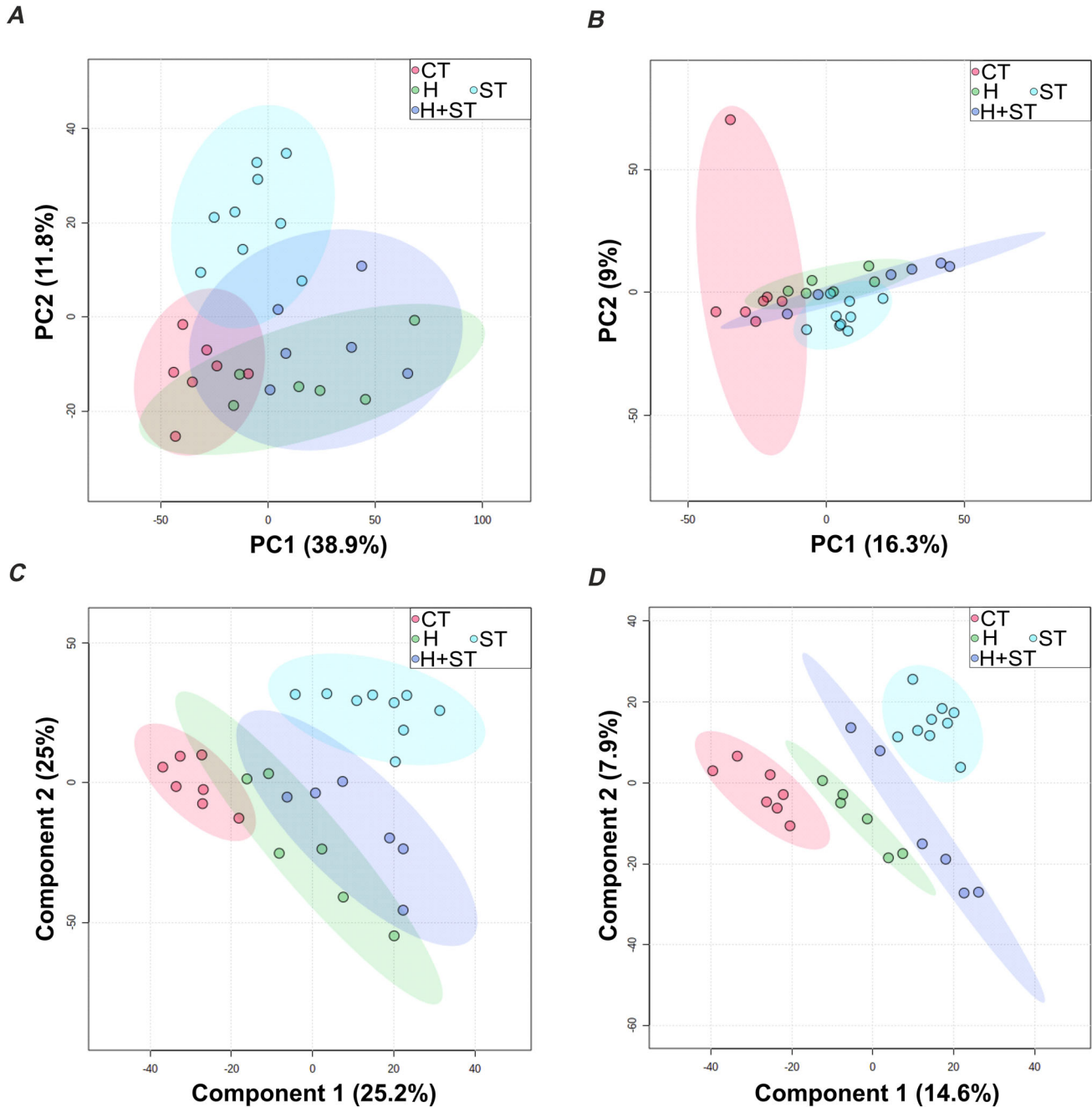


Figure 3. Multivariate analysis for all ion features detected by mass spectrometry

Untargeted metabolomics analysis for reverse-phase LC-MS (underivatized) (A) and (C) and derivatised reverse-phase LC-MS (derivatised) (B) and (D) chromatographic analysis. Data analysed by principal component analysis (A) and (B) and partial-least squares discriminant analysis (PLS-DA) (C) and (D) to determine the similarity between measured and modelled data (data represents $n = 6-9$ samples/group). Data for PLS-DA represents a direct comparison of experimental data with modelled data, exploiting permutation analysis to determine the integrity of the data.

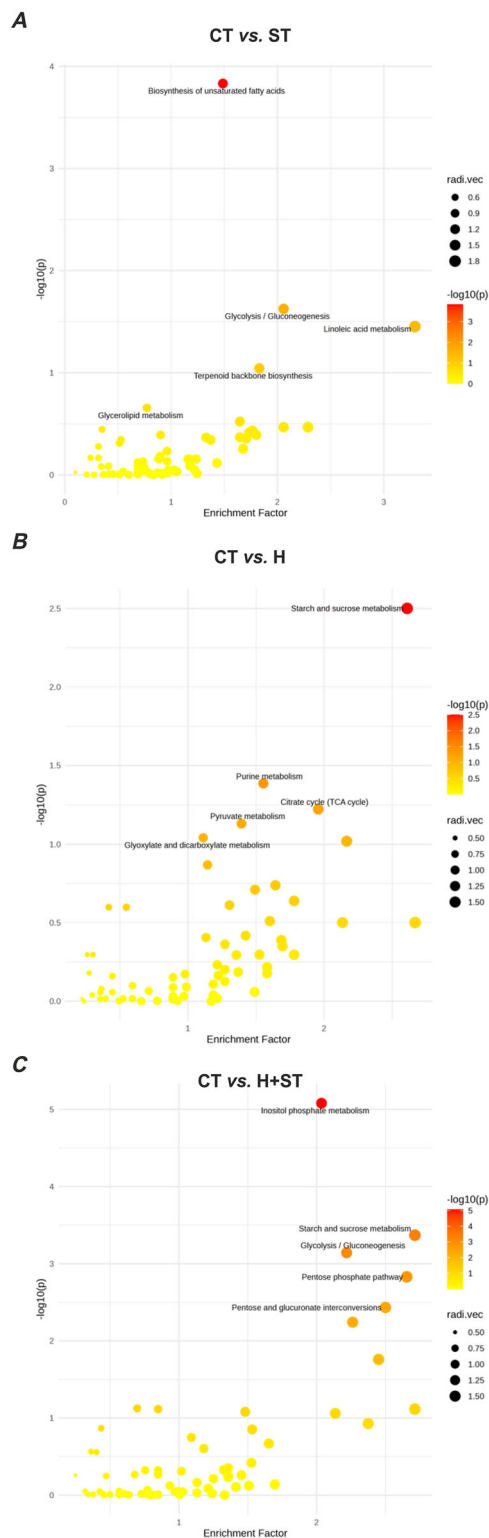


Figure 4. Pathway analysis for unidentified ion-features from reverse-phase chromatography LC-MS to determine putative targets for pathway investigation

All ion-features were included and fold change (t score) and statistical significance (P value) were calculated. Data were analysed

using MetaboAnalyst 5.0 (<https://www.metaboanalyst.ca>). For further details see methods. Significance threshold was set at $P < 0.05$; species selection was for mouse (*Mus musculus*) using the Kyoto Encyclopedia of Genes and Genomes (KEGG) (<https://www.genome.jp/kegg>) pathways; pathway identification threshold was set at three metabolites within pathway with a mass cutoff for putative identification = 5 ppm. Data presented for (A) ST, (B) H and (C) H+ST relative to CT. CT, control; H, hypoxia; H+ST, combination indirect stimulation and hypoxia; ST, indirect stimulation.

hypoxia produced a significant decrease (0.51 ± 0.16 FC, $P < 0.001$), with the combination also showing a significant decrease compared to control (0.56 ± 0.11 FC, $P < 0.001$) and stimulation alone ($P = 0.003$). Fructose 1,6-bisphosphate was similarly affected (LMM $F_{3,22,112} = 7.417$, $P_{\text{adj}} = 0.003$) (Fig. 6C) with H+ST significantly reducing levels compared to control (0.51 ± 0.18 FC, $P < 0.001$) and to ST alone ($P = 0.003$). Hypoxia modulated the next two stages in glycolysis: dihydroxyacetone phosphate (LMM $F_{3,9,743} = 8.404$, $P_{\text{adj}} = 0.009$) (Fig. 6D) and glyceraldehyde 3-phosphate (LMM $F_{3,5,687} = 10.271$, $P_{\text{adj}} = 0.017$) (Fig. 6E). Levels of dihydroxyacetone phosphate were reduced compared to controls (0.46 ± 0.08 FC, $P = 0.003$) and ST (1.06 ± 0.39 FC, $P < 0.001$), with a comparable response in H+ST (Fig. 6D). Similarly, glyceraldehyde-3-phosphate levels were significantly reduced in the combination group compared to control levels (0.70 ± 0.10 FC, $P < 0.001$) (Fig. 6E). Interestingly, elevated levels of 1,3-bisphosphoglycerate (LMM $F_{3,24,241} = 14.525$, $P_{\text{adj}} < 0.001$) (Fig. 6F) were present in the H+ST group (1.32 ± 0.26 FC, $P < 0.001$), whereas H resulted in a significant decrease (0.79 ± 0.07 FC, $P = 0.015$). A differential response in 3-phosphoglycerate (LMM $F_{3,28} = 5.886$, $P_{\text{adj}} = 0.007$) (Fig. 6G) between ST and H (0.76 ± 0.33 vs. 1.25 ± 0.48 FC, respectively, $P = 0.049$) culminated in unmoderated levels following H+ST (0.55 ± 0.33 FC, $P = 1.03$) (Fig. 6G). Pyruvate remained unchanged (LMM $F_{3,4,618} = 5.842$, $P_{\text{adj}} = 0.059$) (Fig. 6H). Finally, acetyl-CoA (LMM $F_{3,16,95} = 5.744$, $P_{\text{adj}} = 0.012$) (Fig. 6I) levels were significantly modified, with skeletal muscle exposed to H having significantly higher levels (2.97 ± 1.177 FC, $P = 0.005$) (Fig. 6I) compared to control and to ST (1.13 ± 0.88 FC, $P = 0.005$); further H+ST also presented with significantly elevated levels of acetyl-CoA compared to control levels (H+ST, 2.59 ± 1.00 FC, $P = 0.016$) and compared to ST ($P = 0.016$).

Branched chain amino acids. Branched amino acids can contribute to central energy metabolism through transamination reactions and the formation of ketoacids (Fig. 7A). As seen above, there was significant modulation of fructose 6-phosphate (Fig. 6B), fructose

1,6-bisphosphate (Fig. 6C), pyruvate (Fig. 6H) and acetyl-CoA (Fig. 6I) within this pathway. The product, citric acid, was significantly modulated overall (LMM $F_{3,28} = 4.084$, $P_{\text{adj}} = 0.024$) (Fig. 7B), largely due to a reduction following ST (0.70 ± 0.22 FC, $P = 0.020$). Skeletal muscle levels of valine (LMM $F_{3,28} = 14.403$, $P_{\text{adj}} < 0.001$) (Fig. 7C), isoleucine (LMM $F_{3,28} = 10.465$, $P_{\text{adj}} < 0.001$) (Fig. 7D) and leucine (LMM $F_{3,28} = 17.758$, $P_{\text{adj}} < 0.001$) (Fig. 7E) were all significantly modulated following oxygen kinetic manipulation. Indirect stimulation (0.71 ± 0.14 FC, $P < 0.001$), H (0.61 ± 0.15

FC, $P < 0.001$) and H+ST (0.51 ± 0.18 , $P < 0.001$) significantly lowered levels of valine (Fig. 7C). Similarly, isoleucine presented with significantly decreased levels in response to ST (0.69 ± 0.17 FC, $P < 0.001$), H (0.61 ± 0.16 FC, $P < 0.001$) and H+ST (0.58 ± 0.20 FC, $P < 0.001$) compared to control (Fig. 7D). Leucine followed the same trend with significant decreases in ST (0.67 ± 0.12 FC, $P < 0.001$), H (0.53 ± 0.14 FC, $P < 0.001$) and H+ST groups (0.49 ± 0.22 FC, $P < 0.001$) relative to control (Fig. 7E).

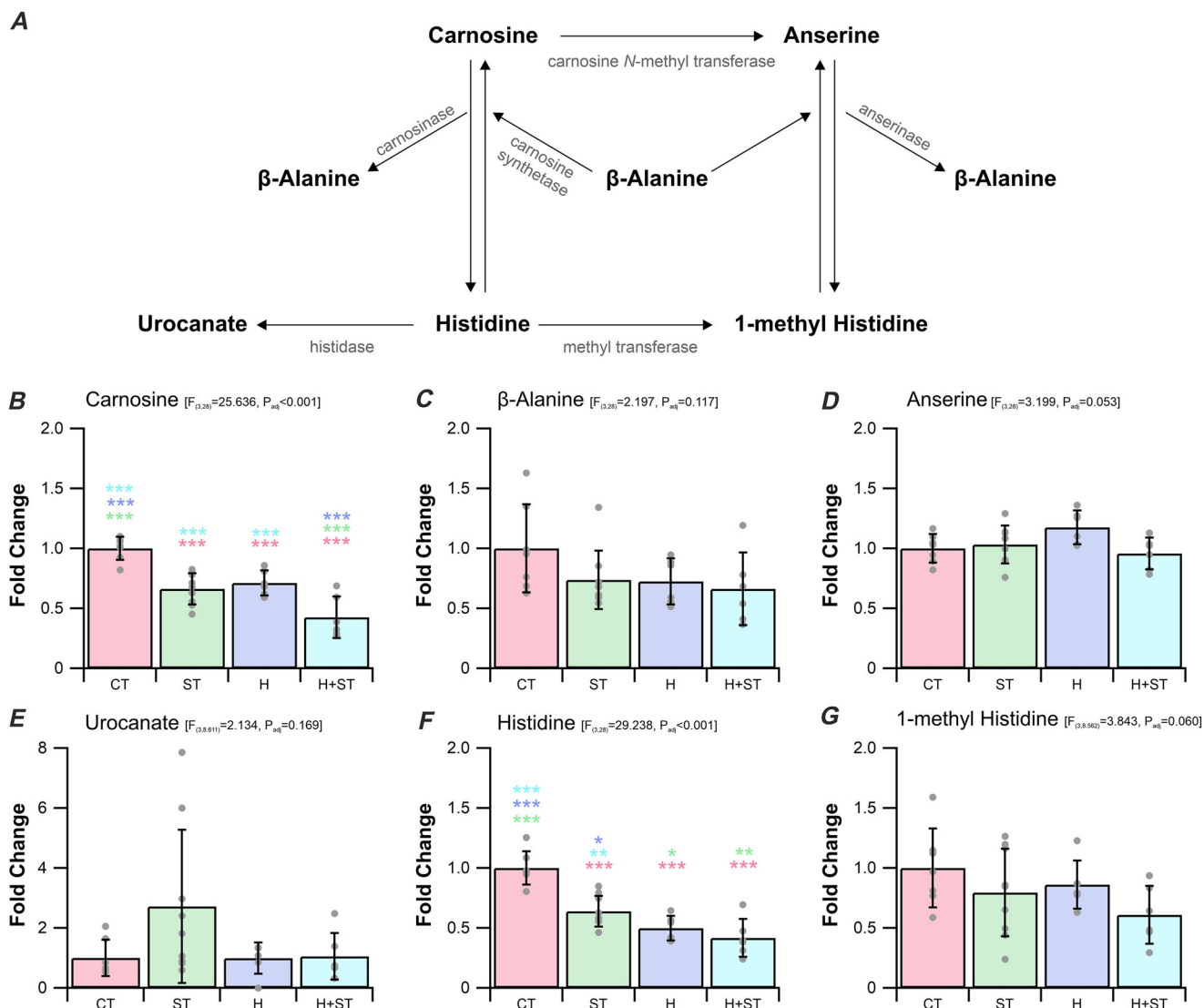


Figure 5. The effect of differential manipulation of local tissue oxygen levels on the metabolism of histidine and 1-methyl histidine in the tibialis anterior

Metabolite mapped onto the metabolic pathway (A). Although no significant modulation of β -alanine (C), anserine (D), urocanate (E) and 1-methyl histidine (G) was present, there was a significant reduction in carnosine (B) and histidine (F) across treatment groups. Data are presented as the mean \pm SD, * $P \leq 0.05$, ** $P \leq 0.01$, *** $P \leq 0.001$. Control (CT, $n = 7$), indirect stimulation (ST, $n = 9$), hypoxia (H, $n = 6$) and combination indirect stimulation and hypoxia (H+ST, $n = 6$).

Discussion

There has been controversy about the structural (capillary) response of skeletal muscle to altered tissue O₂ levels (Lemieux & Birot, 2021), involving decreased supply (hypoxia) or increased demand (activity), partly

as a result of methodological issues (Ahmed et al. 1997, Deveci et al. 2001; Kissane & Egginton 2019). The use of a mouse model may help further this debate. We demonstrate that, as anticipated (hypothesis 1), activation of skeletal muscle in mice by indirect electrical

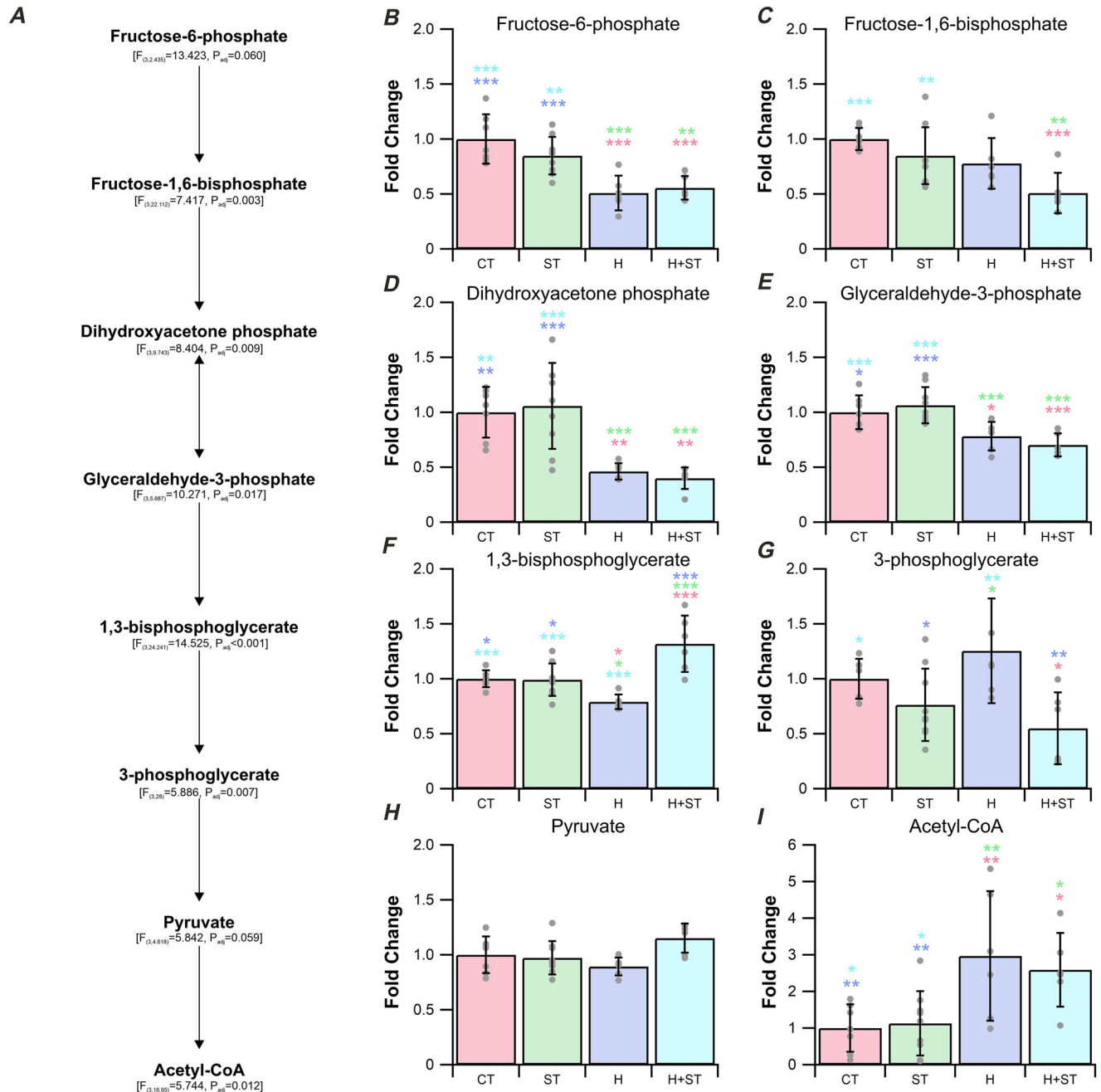


Figure 6. The effect of differential manipulation of local tissue oxygen levels on glycolysis metabolism Metabolite mapped onto the glycolysis metabolic pathway with linear mixed model statistics (A). Differential regulation occurred throughout the glycolysis pathway with significant differences seen in fructose 6-phosphate (B), fructose 1,6-bisphosphate (C), dihydroxyacetone phosphate (D), glyceraldehyde 3-phosphate (E), 1,3-bisphosphoglycerate (F), 3-phosphoglycerate (G), pyruvate (H) and acetyl-CoA (I) levels. Data are presented as the mean \pm SD, * $P \leq 0.05$, ** $P \leq 0.01$, *** $P \leq 0.001$. Control (CT, $n = 7$), indirect stimulation (ST, $n = 9$), hypoxia (H, $n = 6$) and combination indirect stimulation and hypoxia (H+ST, $n = 6$).

stimulation (ST) led to significant expansion of the capillary bed in the TA. However, a similar adaptive structural response was not observed following hypoxia (H), and, when combined with ST, H appears to blunt the structural remodelling. Therefore, complementary structural changes to muscle induced by increased activity and reduced O₂ availability are not observed. By contrast, we hypothesised (hypothesis 2) that the mainly mechanotransductive (ST) and largely chemotransductive (H) stimuli were able to independently manipulate the metabolic status of muscle. Specifically, H led to changes in glycolytic metabolites, indicative of increased reliance of substrate level phosphorylation for the synthesis of ATP. Interestingly, when both stimuli were combined (H+ST), there was a further decrease in tissue fructose 1,6-bisphosphate levels, indicating that, although no structural remodelling was evident to facilitate supply of O₂ delivery and substrate mobilisation, metabolic realignment was observed. Interestingly, ST alone showed no effect on glycolytic metabolite levels, suggesting that any structural adaptation leading to greater capillary supply was sufficient to sustain the metabolic character of the muscle.

Hypoxia blunts microvascular bed expansion

Although ST is a potent angiogenic driver across the TA muscle, the core was affected to a greater extent than the cortex, suggesting that the oxidative region is closer to functional supply capacity and hence required structural adaptation to accommodate greater activity. This is the first time that this ST paradigm has been used in mice, although these data are consistent with much of the previous literature in rats (Kissane et al., 2023; Linderman et al., 2000), highlighting the utility of low-frequency stimulation as an angiogenic driver. The current data suggest that 1 week of hypoxia is insufficient to drive microvascular remodelling, although there is little agreement on the angiogenic potential of H alone (Lemieux & Birot, 2021). Although we showed that a compartmental adaptive response is present after 3 weeks of H in rat TA (Deveci et al., 2001), others suggest that after 8 weeks (Olfert et al., 2001) or 12 weeks (Bigard et al., 1991) of chronic hypoxia, there was no change in C:F across many of the hindlimb muscles of the rat, whereas exercising for these lengths of time did lead to significant increases in C:F. The combination of H+ST in our hands significantly blunted the angiogenic response (specifically

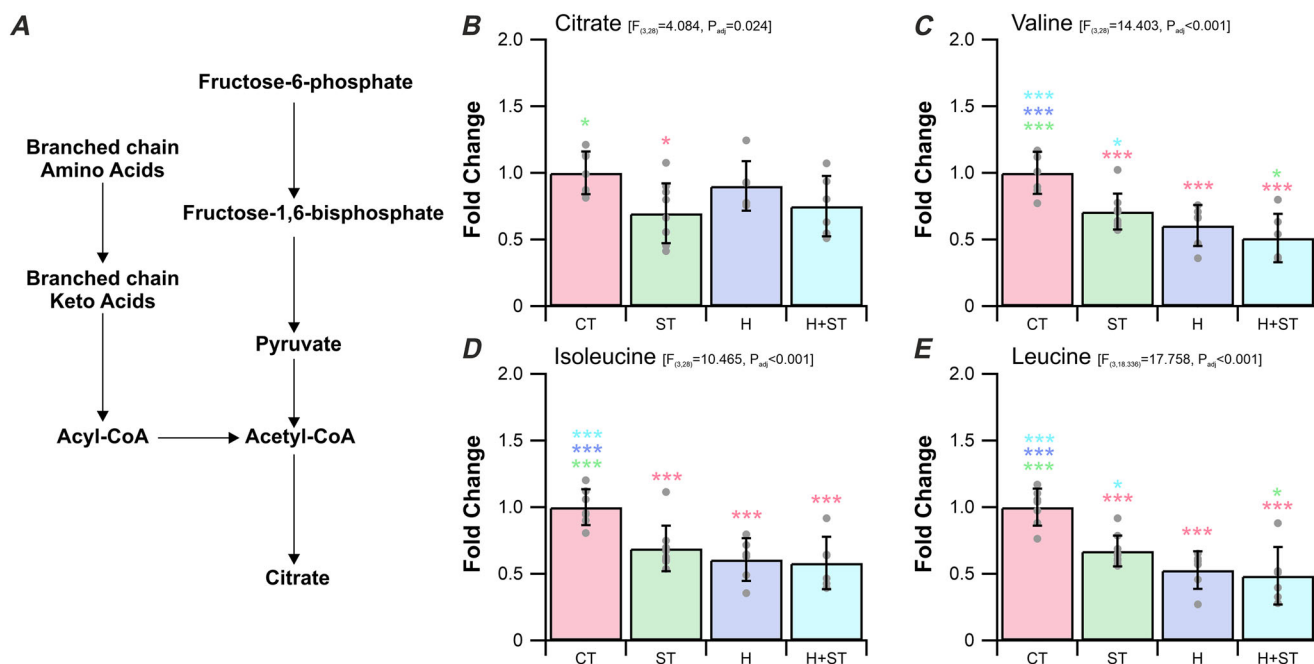


Figure 7. The effect of differential manipulation of local tissue oxygen levels on branch chain amino acid metabolism

Metabolite mapped onto metabolic pathway highlighting changes to branched chain amino acid (BCAA) metabolism for energy production (A). Significant differences occurred throughout the BCAA pathway, specifically, citrate (B), valine (C), isoleucine (D) and leucine (E). Data are presented as the mean \pm SD, * $P \leq 0.05$, ** $P \leq 0.01$, *** $P \leq 0.001$. Control (CT, $n = 7$), indirect stimulation (ST, $n = 9$), hypoxia (H, $n = 6$) and combination indirect stimulation and hypoxia (H+ST, $n = 6$).

CD) seen across the TA compared to ST alone. By contrast, exercise training in combination with H significantly improved microvascular composition in rats compared to the levels achieved with exercise alone, with concomitant decreases in muscle VEGF abundance or receptor mRNA expression (Flt-1 or Flk-1) (Olfert et al., 2001). This may partly explain why, in our H+ST group, there was a reduced expansion of capillary supply, as inhibition of VEGF has been shown to blunt the angiogenic response of two of the main mechanotransductive pathways (Hoier & Hellsten, 2014; Williams, Cartland, Rudge, et al., 2006).

Mechanotransductive and chemotransductive pathways converge on histidine metabolism

Both ST and H significantly reduced levels of carnosine and histidine, which appears to be further exacerbated when these stimuli are combined, suggesting that muscle tolerance of acidosis may be decreased, because pH control has been associated with both metabolites (Abe, 2000). These data mirror findings in humans following intense exercise that show decreased muscle buffering capacity and a low protein buffering capacity involving histidine and carnosine (Bishop et al., 2009), which may directly impact shifts in glycolysis pathway associated with increased lactic acid production. Furthermore, given the proximity of the pK_a ($pK_a = 6-7$) for the imidazole residue on histidine or carnosine to muscle pH during intense exercise ($pK_a = 6.8$) (Bangsbo et al., 1996; Street et al., 2001), this suggests that the decreases in these amino acids may also adversely affect rates of resynthesis for phosphocreatine and thus impair muscle endurance (McMahon & Jenkins, 2002). However, haematopoiesis associated with chronic hypoxia may yield increased haemoglobin-buffering of muscle pH changes, ameliorating effects of possible acidosis (Juel et al., 2003).

Hypoxia differentially modifies glycolysis metabolism

Proximate portions of the glycolytic pathway were impacted following hypoxia, suggesting that H had the effect of decreasing overall metabolite levels, whereas the mechanotransductive signals had no such effect. Therefore, H placed a significant metabolic burden on the TA for ATP production. Early human experiments highlighted the potency of acute electrical stimulation of muscle to increase rates of glycolysis (Ren et al., 1988). Similarly, rat ST experiments demonstrated a significant increase in CD in the absence of changes to enzyme activities, including succinate dehydrogenase and cytochrome oxidase, for functions of central energy metabolism (Egginton & Hudlicka, 2000). In hypoxia, the terminal electron acceptor (i.e. O_2) is decreased, therefore limiting oxidative phosphorylation, so that, to

sustain production of ATP, increased reliance on substrate level phosphorylation is necessary, yielding a decrease in glycolytic substrates. In humans, chronic hypoxia led to increased expression of complex II and complex IV of the electron transport chain, thereby improving aerobic performance (Desplanches et al., 2014), although H led to diminished rates of mitochondrial oxidation in skeletal muscle *in vitro* (Gamboa & Andrade, 2012) associated with decreased aconitase activity (Magalhães et al., 2005). This is consistent with increased acetyl-CoA following H in the present study because C2 units are not moved on to the TCA cycle; hence, TA muscle citrate levels were unaffected by ST or H. We also showed decreased TA levels of fructose 6-phosphate, fructose 1,6-bisphosphate and dihydroxyacetone phosphate, indicating increased utilisation of glucose metabolites, leading to elevated tissue acetyl-CoA levels. Similarly in humans, high altitude hypoxia increased both glycolytic and TCA cycle intermediate abundances, coupled with decreased abundances for BCAA (including leucine, isoleucine and valine), thus implicating BCAA breakdown in energy provision (Margolis et al., 2021), consistent with our current observations.

The absence of an additive angiogenic effect for ST in combination with H may have a metabolic origin. Previous studies highlight that sprouting angiogenesis requires functional endothelial cell glycolysis for the production of ATP, for which the rate-limiting step was production of fructose 1,6-bisphosphate (De Bock et al., 2013), and inhibition of PFKFB3 led to blunting of the angiogenic response to H (Schoors et al., 2014). We report a significant decline in muscle fructose 1,6-bisphosphate levels following the combination of H+ST, again implying that availability of substrates for the synthesis of ATP through substrate level phosphorylation may be limited, thus reducing angiogenic potential. However, it must be acknowledged that the principal fate of fructose 1,6-bisphosphate is fuelling glycolysis; hence tissue concentrations are subject to fluctuation based on muscle activity, and thus direct effects on angiogenesis may be limited *in vivo*.

Exercise enhances branch chain amino acid metabolism

Both exercise-simulated mechanotransduction (via indirect stimulation) and chemotransduction (response to hypoxia) elevated skeletal muscle BCAA metabolism, which was sustained in the combination treatment group. Both exercise and hypoxia have the potential to decrease muscle free amino acid concentrations (Gabrys et al., 2003), with our data consistent with both stimuli alone increasing requirements for BCAAs and thus increased protein synthesis (Kimball et al.,

2002; Shimomura et al., 2004). An anabolic response would be needed for structural remodelling, and possibly metabolic realignment. However, it may also reflect an increased metabolic requirement for ATP, and hence an energy deficit (She et al., 2010). Our data extend such observations and imply that BCAAs contributed to central energy metabolism, probably as a result of relative energy deprivation for the synthesis of ketoacids and acyl-CoA to support metabolism (Bailey et al., 2001). BCAAs may augment energy production with the incorporation of keto-acids to the distal portions of the glycolytic cycle to increase acetyl-CoA flux through the TCA cycle and maintain ATP production (Mikalayeva et al., 2021). Interestingly, cell culture experiments have demonstrated that, for glioblastoma cells, hypoxia increased expression of branched-chain amino acid transporter proteins in a hypoxia-inducible factor (HIF)-1 α -dependent manner (Zhang et al., 2021), suggesting a mechanism facilitating increased BCAA uptake in muscle. HIF-1 α also plays a key role in differentially regulating angiogenesis during physiological remodelling (Egginton 2009). A role for amino acids in the control of angiogenesis may also contribute to the lack of change in capillarity observed following combining H and ST, where for example, free glycine is required for VEGF-induced angiogenesis (Guo et al., 2017).

Scaling of oxygen supply and metabolic pathways: a tale of caution?

Rodents are often the first-choice experimental animal in physiology research as a result of their substantially well characterised genome and a capacity to genetically modify for experimental research. However, these animals are not always an ideal surrogate for human physiological and pathophysiological research. For example, the guinea-pig presents with the greatest similarity in transcriptional and muscle wasting response in a smoking induced COPD model (Davidsen et al., 2014), although rats and mice still dominate this particular research sphere. In a similar vein, the scaling of oxygen supply and muscle phenotype must be considered in our interpretations of the data presented for mice, when comparing with larger species such as rats and humans, where orders of magnitude greater diffusion distances are involved (Egginton, 1990; Kissane & Egginton, 2019; Queeno et al., 2023). We have compared our previously published data on rat TA that have undergone an identical indirect stimulation paradigm (Kissane et al., 2023), to highlight the differences across scales (see Appendix, Figs A2–A4).

First, our data show that both mice and rats respond to ST in the same adaptive directions (e.g. both present with increases in CD, C:F and reduced CDA) across the oxidative core (see Appendix, Fig. A2) and

glycolytic cortex (see Appendix, Fig. A3). Despite mice having inherently smaller intramuscular and intracellular diffusion distances (higher CD and lower FCSA, respectively), and greater oxidative phenotype (Queeno et al., 2023), they still present with an increased oxygen supply network. Where there is evidence of angiogenesis (increased C:F), the functionally relevant index of supply capacity (CD) is influenced by FCSA. This is most evident in the glycolytic cortex, where the extent of hypoxia during exercise is estimated to be greater, reflecting the larger fibre size. Interestingly, despite similarities in structural remodelling across these two species, the metabolic adaptation to ST differed (specifically the histidine/methyl-histidine pathway; see Appendix, Fig. A4). Mice demonstrated a significant reduction in levels of histidine and carnosine, potentially impacting muscle tolerance of acidosis, which may directly impact shifts in glycolysis pathway. Rats did not display such a reduction in carnosine or histidine; rather, a distinct elevation of methyl-histidine levels may reflect the degree of transition during ST, implying that muscle remodelling may be incomplete (Kissane et al., 2023) and suggesting that a more sustained stimulus is required to reach equilibrium in the rat skeletal muscle.

Caution is needed when extrapolating findings across scales, and our previous experiments manipulating levels of mechanotransduction in rats (Kissane et al., 2023) support a graded metabolic response for individual metabolites, probably linked to tissue oxygen gradients (Walenta et al., 2001). This may be a consequence of species differences, involving varying metabolic rates and oxygen diffusion distances (Schmidt-Nielsen & Pennycuik, 1961). Additionally, species-specific responses to angiogenic stimuli have been presented previously (Norrby et al., 1989), with rats showing greater vascular remodelling for lung vasculature in response to chronic hypoxia compared to mice (Hoshikawa et al., 2003).

Limitations and future direction

Although there is evidence that the chronic combination of exercise and hypoxia (≥ 3 weeks) may drive greater adaptive structural remodelling of the microvasculature compared to training at normoxia, it is not known whether this combined training response may happen earlier (Lemieux & Birot, 2021). Here, we have provided insight at a single, acute timepoint, suggesting that hypoxia may in fact blunt the training adaptive response. These observations imply that a metabolic response to physiological challenge, normally assumed to be relatively quick, may lag other compensatory mechanisms. However, if insufficient, this may subsequently drive structural adaptations to facilitate an adequate holistic response. To further validate this assertion, it is necessary to undertake

more refined acute-to-chronic timepoint measurements to clarify such interaction.

Furthermore, we have used ST as an exercise surrogate. First, for its reproducible muscle workloads, and second, because indirect stimulation at 10 Hz has been shown to promote the greatest active hyperaemia response at a submaximal force recruitment, leading to significantly elevated microvascular composition across the TA (Kissane et al., 2023). In this model, we expect the intracellular P_{O_2} during muscle activity to be close to estimates during exercise ($\sim 1\text{--}5$ mmHg) (Poole & Musch, 2023), supporting its physiological validity and surrogacy for traditional exercise interventions in rodents. The impact of a cyclic (transient) muscle activation pattern, and therefore the potential for a transient tissue hypoxia cannot be ruled out. However, a transient decrease in P_{O_2} is probably accommodated by physiological capacitance, namely resistance to normal fluctuations in supply and demand, whereas hypoxia-induced responses require some (often indeterminate) period of exposure before triggering an adaptive response.

Conclusions

In the present study, we have demonstrated functionally relevant skeletal muscle adaptation to mechanotransduction-driven angiogenesis through acute indirect stimulation. However, counter to our hypothesis 1, hypoxia did not promote a similar structural remodelling that would facilitate greater local oxygen supply. Interestingly, opposed to our hypothesis 2, although ST led to structural remodelling it preserved metabolite levels, H led to greater metabolic realignment in the absence of complementary structural changes.

Understanding the temporal sequence of these events may lead to better muscle interventions to prevent surgical- or disease-induced muscle insult and may be best exploited combining strategies to incorporate both transcriptomics and metabolomics.

Appendix

Fig. A1–A4

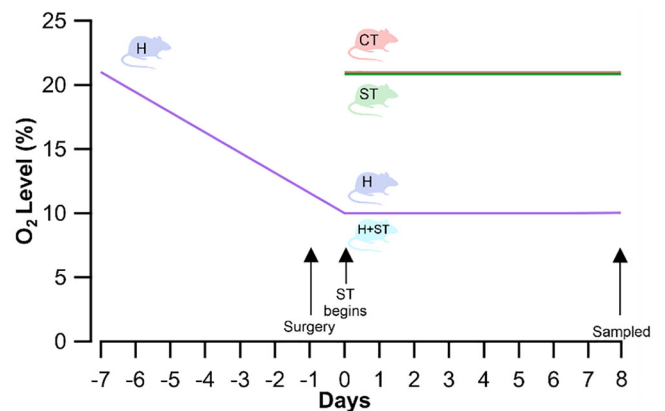


Figure A1. Oxygen levels across the experimental groups

Overview of the experimental timeframe and the oxygen levels of the mice used in the present study. The hypoxia group of mice were gradually lowered over the course of 1 week (Davidsen et al., 2016). Surgery to implant stimulators was completed and turned on 24 h later. Therefore, mice received hypoxia (10%) for 7 days (hypoxia group; H) on their contralateral limb, while the ipsilateral limb received hypoxia and indirect stimulation (H+ST). A control group of mice underwent no surgery (CT), whereas the stimulation only mice received 7 days of indirect stimulation (ST).

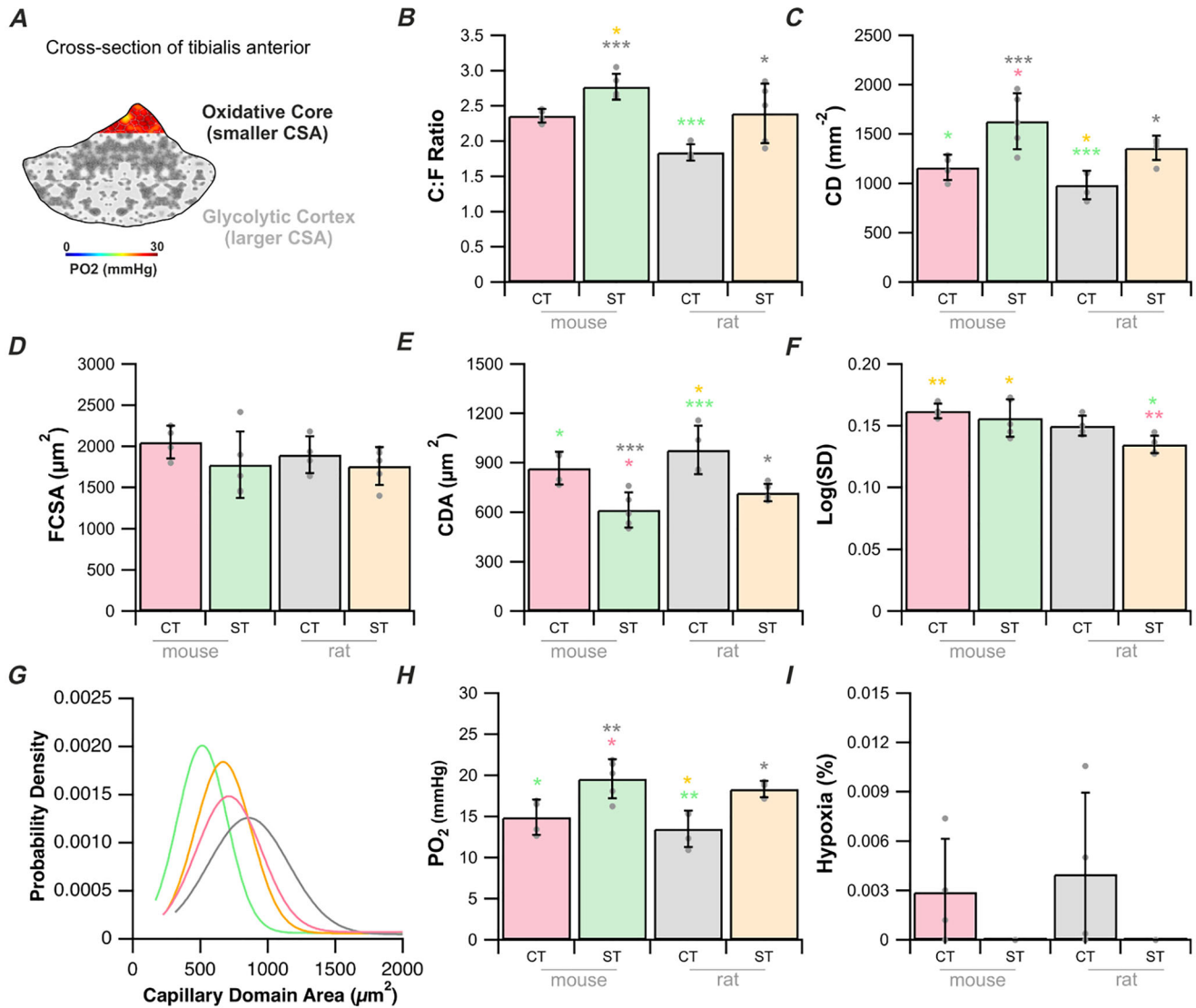


Figure A2. Angiogenic response of the tibialis anterior core region across scales

The posterior compartment of the tibialis anterior contains smaller and more oxidative fibres in both mice and rats (A). Changes in capillary-to-fibre ratio (B), capillary density (C), fibre cross-sectional area (D), capillary domain area (E), standard deviation of the logged capillary domain area (F) and (G), modelled tissue P_{O_2} (H) and estimated hypoxia (I) for the core region of the tibialis anterior in response to indirect electrical stimulation. Data are presented as the mean \pm SD, * $P \leq 0.05$, ** $P \leq 0.01$, *** $P \leq 0.001$. Control (CT; mouse $n = 4$, rat $n = 4$), indirect stimulation (ST, mouse $n = 5$, rat $n = 5$).

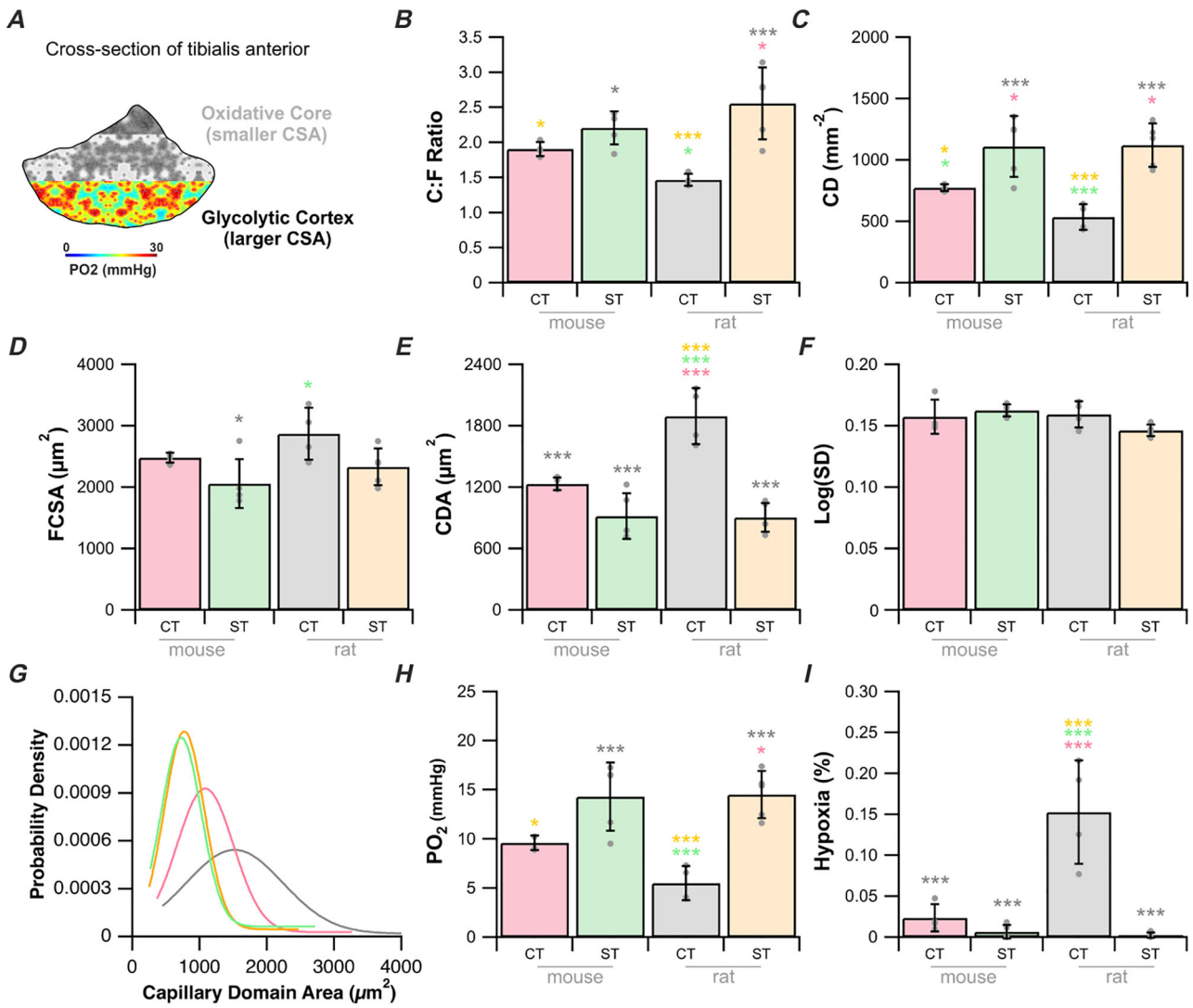


Figure A3. Angiogenic response of the tibialis anterior cortex region across scales

The anterior compartment of the tibialis anterior contains larger and more glycolytic fibres in both mice and rats (A). Changes in capillary-to-fibre ratio (B), capillary density (C), fibre cross-sectional area (D), capillary domain area (E), standard deviation of the logged capillary domain area (F) and (G), modelled tissue P_{O₂} (H), and estimated hypoxia (I) for the core region of the tibialis anterior in response to indirect electrical stimulation. Data are presented as the mean ± SD, *P ≤ 0.05, **P ≤ 0.01, ***P ≤ 0.001. Control (CT; mouse n = 4, rat n = 4), indirect stimulation (ST, mouse n = 5, rat n = 5).

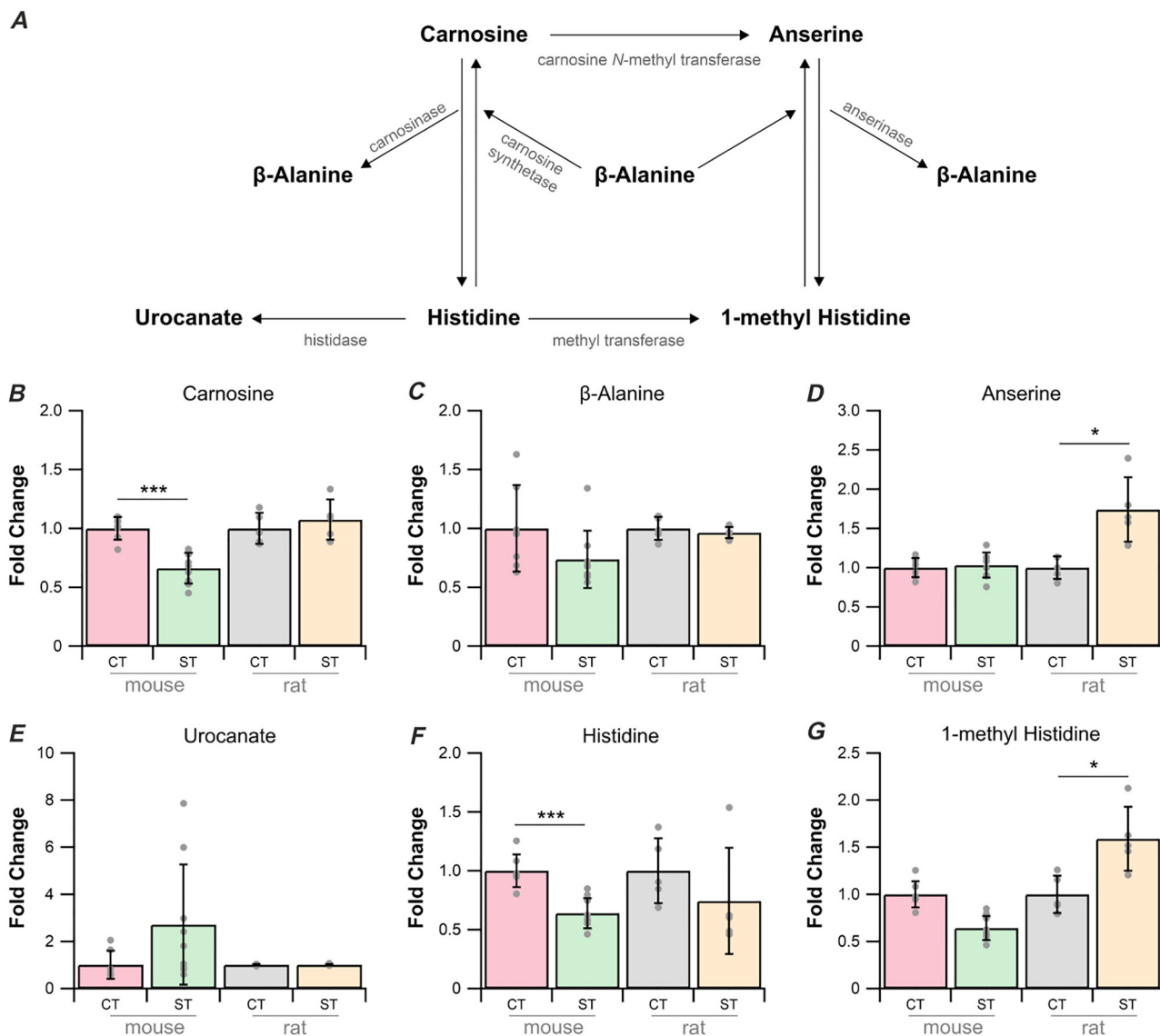


Figure A4. The differential effect of indirect electrical stimulation on the metabolism of histidine and 1-methyl histidine across mice and rats

Metabolite mapped onto the metabolic pathway (A). Mice predominantly presented with modified levels of carnosine (B) and histidine (F), whereas rat skeletal presented with increased anserine (D) and 1-methyl histidine (G). Across both species β -alanine (C) and urocanate (E) were not significantly different. Data are presented as the mean \pm SD, * $P \leq 0.05$, ** $P \leq 0.01$, *** $P \leq 0.001$ vs. species-specific control. Control (CT; mouse $n = 7$, rat $n = 5$) and indirect stimulation (ST; mouse $n = 9$, rat $n = 5$).

References

- Abe, H. (2000). Role of histidine-related compounds as intracellular proton buffering constituents in vertebrate muscle. *Biochemistry C/C of Biokhimiia*, **65**, 757–765.
- Ahmed, S., Egginton, S., Jakeman, P., Mannion, A., & Ross, H. (1997). Is human skeletal muscle capillary supply modelled according to fibre size or fibre type? *Experimental Physiology*, **82**, 231–234.
- Al-Shammari, A. A., Kissane, R. W. P., Ashkanani, A., Madhoun, A. A., Al-Mulla, F., Gaffney, E. A., & Egginton, S. (2025). Utility of local capillary supply indices: Insights from computational image-based modelling. *The Journal of Physiology*. Advance online publication. <https://doi.org/10.1113/JP288043>
- Al-Shammari, A. A., Kissane, R. W. P., Holbek, S., Mackey, A. L., Andersen, T. R., Gaffney, E. A., Kjaer, M., & Egginton, S. (2019). Integrated method for quantitative morphometry and oxygen transport modeling in striated muscle. *Journal of Applied Physiology*, **126**, 544–557.
- Bailey, D. M., Davies, B., Castell, L. M., Newsholme, E. A., & Calam, J. (2001). Physical exercise and normobaric hypoxia: Independent modulators of peripheral cholecystokinin metabolism in man. *Journal of Applied Physiology*, **90**(1), 105–113.
- Bangsbo, J., Madsen, K., Kiens, B., & Richter, E. (1996). Effect of muscle acidity on muscle metabolism and fatigue during intense exercise in man. *The Journal of Physiology*, **495**(2), 587–596.
- Bigard, A. X., Brunet, A., Guezennec, C.-Y., & Monod, H. (1991). Effects of chronic hypoxia and endurance training on muscle capillarization in rats. *Pflügers Archiv*, **419**(3–4), 225–229.
- Bishop, D., Edge, J., Mendez-Villanueva, A., Thomas, C., & Schneiker, K. (2009). High-intensity exercise decreases muscle buffer capacity via a decrease in protein buffering in human skeletal muscle. *Pflügers Archiv-European Journal of Physiology*, **458**(5), 929–936.
- Buchegger, A., Nemeth, P. M., Pette, D., & Reichmann, H. (1984). Effects of chronic stimulation on the metabolic heterogeneity of the fibre population in rabbit tibialis anterior muscle. *The Journal of Physiology*, **350**(1), 109–119.
- Davidson, P. K., Herbert, J. M., Antczak, P., Clarke, K., Ferrer, E., Peinado, V. I., Gonzalez, C., Roca, J., Egginton, S., Barberá, J. A., & Falciani, F. (2014). A systems biology approach reveals a link between systemic cytokines and skeletal muscle energy metabolism in a rodent smoking model and human COPD. *Genome Medicine*, **6**(8), 59.
- Davidson, P. K., Turan, N., Egginton, S., & Falciani, F. (2016). Multilevel functional genomics data integration as a tool for understanding physiology: A network biology perspective. *Journal of Applied Physiology*, **120**(3), 297–309.
- De Bock, K., Georgiadou, M., Schoors, S., Kuchnio, A., Wong, B. W., Cantelmo, A. R., Quaegebeur, A., Ghesquière, B., Cauwenberghs, S., Eelen, G., Phng, L.-K., Betz, I., Tembuyser, B., Brepoels, K., Welti, J., Geudens, I., Segura, I., Cruys, B., Bifari, F., ... Carmeliet, P. (2013). Role of PFKFB3-driven glycolysis in vessel sprouting. *Cell*, **154**(3), 651–663.
- Desplanches, D., Amami, M., Dupré-Aucouturier, S., Valdivieso, P., Schmutz, S., Mueller, M., Hoppeler, H., Kreis, R., & Flück, M. (2014). Hypoxia refines plasticity of mitochondrial respiration to repeated muscle work. *European Journal of Applied Physiology*, **114**(2), 405–417.
- Deveci, D., Marshall, J., & Egginton, S. (2002). Chronic hypoxia induces prolonged angiogenesis in skeletal muscles of rat. *Experimental Physiology*, **87**(3), 287–291.
- Deveci, D., Marshall, J. M., & Egginton, S. (2001). Relationship between capillary angiogenesis, fiber type, and fiber size in chronic systemic hypoxia. *American Journal of Physiology-Heart and Circulatory Physiology*, **281**(1), H241–H252.
- Doody, N. E., Smith, N. J., Akam, E. C., Askew, G. N., Kwok, J. C., & Ichiyama, R. M. (2024). Differential expression of genes in the RhoA/ROCK pathway in the hippocampus and cortex following intermittent hypoxia and high-intensity interval training. *Journal of Neurophysiology*, **132**(2), 531–543.
- Egginton, S. (1990). Morphometric analysis of tissue capillary supply. In *Vertebrate gas exchange* (pp. 73–141). Springer.
- Egginton, S. (2009). Invited review: Activity-induced angiogenesis. *Pflügers Archiv-European Journal of Physiology*, **457**(5), 963–977.
- Egginton, S., & Hudlicka, O. (2000). Selective long-term electrical stimulation of fast glycolytic fibres increases capillary supply but not oxidative enzyme activity in rat skeletal muscles. *Experimental Physiology*, **85**, 567–573.
- Friole, R., Hoppeler, H., & Krähenbühl, S. (1994). Relationship between the coenzyme A and the carnitine pools in human skeletal muscle at rest and after exhaustive exercise under normoxic and acutely hypoxic conditions. *The Journal of Clinical Investigation*, **94**(4), 1490–1495.
- Gabrys, J., Konecki, J., Shani, J., Durczok, A., Bielaczyc, G., Kosteczko, A., Szewczyk, H., & Brus, R. (2003). Proteinous amino acids in muscle cytosol of rats' heart after exercise and hypoxia. *Receptors and Channels*, **9**(5), 301–307.
- Gamboa, J. L., & Andrade, F. H. (2012). Muscle endurance and mitochondrial function after chronic normobaric hypoxia: Contrast of respiratory and limb muscles. *Pflügers Archiv-European Journal of Physiology*, **463**(2), 327–338.
- Gondin, J., Brocca, L., Bellinzona, E., d'Antona, G., Maffiuletti, N. A., Miotti, D., Pellegrino, M. A., & Bottinelli, R. (2011). Neuromuscular electrical stimulation training induces atypical adaptations of the human skeletal muscle phenotype: A functional and proteomic analysis. *Journal of Applied Physiology*, **110**(2), 433–450.
- Grundy, D. (2015). *Principles and standards for reporting animal experiments in The Journal of Physiology and Experimental Physiology* (pp. 755–758). Wiley Online Library.
- Guo, D., Murdoch, C. E., Xu, H., Shi, H., Duan, D. D., Ahmed, A., & Gu, Y. (2017). Vascular endothelial growth factor signaling requires glycine to promote angiogenesis. *Scientific Reports*, **7**(1), 14749.
- Hoier, B., & Hellsten, Y. (2014). Exercise-induced capillary growth in Human skeletal muscle and the dynamics of VEGF. *Microcirculation*, **21**(4), 301–314.

- Hoshikawa, Y., Nana-Sinkam, P., Moore, M. D., Sotito-Santiago, S., Phang, T., Keith, R. L., Morris, K. G., Kondo, T., Tuder, R. M., Voelkel, N. F., & Geraci, M. W. (2003). Hypoxia induces different genes in the lungs of rats compared with mice. *Physiological Genomics*, **12**(3), 209–219.
- Juel, C., Lundby, C., Sander, M., Calbet, J., & van Hall, G. (2003). Human skeletal muscle and erythrocyte proteins involved in acid-base homeostasis: Adaptations to chronic hypoxia. *The Journal of Physiology*, **548**(2), 639–648.
- Katayama, K., Yamasaki, H., Ookura, M., Yamamoto, K., Sumie, K., Nishitani, K., Nakaya, Y., Shigesima, K., & Hamada, K. (2018). Effect of percutaneous electrical stimulation of the leg muscles under acute normobaric hypoxic environment on blood glucose concentration. *The Journal of Japan Academy of Health Sciences*, **21**, 23–27.
- Kimball, S. R., Farrell, P. A., & Jefferson, L. S. (2002). Invited review: Role of insulin in translational control of protein synthesis in skeletal muscle by amino acids or exercise. *Journal of Applied Physiology*, **93**(3), 1168–1180.
- Kissane, R. W. P., Al-Shammari, A. A., & Egginton, S. (2021). The importance of capillary distribution in supporting muscle function, building on Krogh's seminal ideas. *Comparative Biochemistry and Physiology Part A: Molecular & Integrative Physiology*, **254**, 110889.
- Kissane, R. W. P., & Egginton, S. (2019). Exercise-mediated angiogenesis. *Current Opinion in Physiology*, **10**, 193–201.
- Kissane, R. W. P., Egginton, S., & Askew, G. N. (2018). Regional variation in the mechanical properties and fibre-type composition of the rat extensor digitorum longus muscle. *Experimental Physiology*, **103**(1), 111–124.
- Kissane, R. W. P., Hauton, D., Tickle, P. G., & Egginton, S. (2023). Skeletal muscle adaptation to indirect electrical stimulation: Divergence between microvascular and metabolic adaptations. *Experimental Physiology*, **108**(6), 891–911.
- Kissane, R. W. P., Tickle, P. G., Doody, N. E., Al-Shammari, A. A., & Egginton, S. (2020). Distinct structural and functional angiogenic responses are induced by different mechanical stimuli. *Microcirculation*, **28**, e12677.
- Kissane, R. W. P., Wright, O., Al'Joboori, Y. D., Marczak, P., Ichiyama, R. M., & Egginton, S. (2019). Effects of treadmill training on microvascular remodeling in the rat after spinal cord injury. *Muscle & Nerve*, **59**(3), 370–379.
- Lavier, J., Beaumann, M., Menétrey, S., Bouzourène, K., Rosenblatt-Velin, N., Pialoux, V., Mazzolai, L., Peyter, A.-C., Pellegrin, M., & Millet, G. P. (2021). High-intensity exercise in hypoxia improves endothelial function via increased nitric oxide bioavailability in C57BL/6 mice. *Acta Physiologica*, **233**(2), e13700.
- Lemieux, P., & Birot, O. (2021). Altitude, exercise, and skeletal muscle angio-adaptive responses to hypoxia: A complex story. *Frontiers in Physiology*, **12**, 735557.
- Li, S., Park, Y., Duraisingham, S., Strobel, F. H., Khan, N., Soltow, Q. A., Jones, D. P., & Pulendran, B. (2013). Predicting network activity from high throughput metabolomics. *PLoS Computational Biology*, **9**(7), e1003123.
- Linderman, J. R., Kloehn, M. R., & Greene, A. S. (2000). Development of an implantable muscle stimulator: Measurement of stimulated angiogenesis and poststimulus vessel regression. *Microcirculation*, **7**(2), 119–128.
- Liu, Y., Christensen, P. M., Hellsten, Y., & Gliemann, L. (2022). Effects of exercise training intensity and duration on skeletal muscle capillarization in healthy subjects: A meta-analysis. *Medicine & Science in Sports & Exercise*, **54**(10), 1714–1728.
- Magalhães, J., Ascensão, A., Soares, J. M., Ferreira, R., Neuparth, M. J., Marques, F., & Duarte, J. A. (2005). Acute and severe hypobaric hypoxia increases oxidative stress and impairs mitochondrial function in mouse skeletal muscle. *Journal of Applied Physiology*, **99**(4), 1247–1253.
- Margolis, L. M., Karl, J. P., Wilson, M. A., Coleman, J. L., Ferrando, A. A., Young, A. J., & Pasiakos, S. M. (2021). Metabolomic profiles are reflective of hypoxia-induced insulin resistance during exercise in healthy young adult males. *American Journal of Physiology-Regulatory, Integrative and Comparative Physiology*, **321**(1), R1–R11.
- McMahon, S., & Jenkins, D. (2002). Factors affecting the rate of phosphocreatine resynthesis following intense exercise. *Sports Medicine*, **32**(12), 761–784.
- Mikalayeva, V., Pankevičiūtė, M., Žvikas, V., Skeberdis, V. A., & Bordel, S. (2021). Contribution of branched chain amino acids to energy production and mevalonate synthesis in cancer cells. *Biochemical and Biophysical Research Communications*, **585**, 61–67.
- Nagahisa, H., & Miyata, H. (2018). Influence of hypoxic stimulation on angiogenesis and satellite cells in mouse skeletal muscle. *PLoS ONE*, **13**(11), e0207040.
- Norrby, K., Jakobsson, A., & Sörbo, J. (1989). Mast-cell secretion and angiogenesis, a quantitative study in rats and mice. *Virchows Archiv B*, **57**(1), 251–256.
- Olfert, I. M., Baum, O., Hellsten, Y., & Egginton, S. (2016). Advances and challenges in skeletal muscle angiogenesis. *American Journal of Physiology-Heart and Circulatory Physiology*, **310**(3), H326–H336.
- Olfert, I. M., Breen, E. C., Mathieu-Costello, O., & Wagner, P. D. (2001). Skeletal muscle capillarity and angiogenic mRNA levels after exercise training in normoxia and chronic hypoxia. *Journal of Applied Physiology*, **91**(3), 1176–1184.
- Percie Du Sert, N., Hurst, V., Ahluwalia, A., Alam, S., Avey, M. T., Baker, M., Browne, W. J., Clark, A., Cuthill, I. C., Dirnagl, U., Emerson, M., Garner, P., Holgate, S. T., Howells, D. W., Karp, N. A., Lazic, S. E., Lidster, K., Maccallum, C. J., Macleod, M., ... Würbel, H. (2020). The ARRIVE guidelines 2.0: Updated guidelines for reporting animal research. *Journal of Cerebral Blood Flow & Metabolism*, **40**(9), 1769–1777.
- Pette, D., & Tyler, K. (1983). Response of succinate dehydrogenase activity in fibres of rabbit tibialis anterior muscle to chronic nerve stimulation. *The Journal of Physiology*, **338**(1), 1–9.
- Poole, D. C., & Musch, T. I. (2023). Capillary-mitochondrial oxygen transport in muscle: Paradigm shifts. *Function*, **4**(3), zqad013.

- Queeno, S. R., Sterner, K. N., & O'Neill, M. C. (2023). Meta-analysis data of skeletal muscle slow fiber content across mammalian species. *Data in Brief*, **50**, 109520.
- Ren, J., Chasiotis, D., Bergström, M., & Hultman, E. (1988). Skeletal muscle glucolysis, glycogenolysis and glycogen phosphorylase during electrical stimulation in man. *Acta Physiologica Scandinavica*, **133**(1), 101–107.
- Richardson, R. S., Wagner, H., Mudaliar, S., Saucedo, E., Henry, R., & Wagner, P. (2000). Exercise adaptation attenuates VEGF gene expression in human skeletal muscle. *American Journal of Physiology-Heart and Circulatory Physiology*, **279**(2), H772–H778.
- Salazar, C., Armenta, J. M., Cortés, D. F., & Shulaev, V. (2012). Combination of an AccQ-Tag-Ultra performance liquid chromatographic method with tandem mass spectrometry for the analysis of amino acids. In M. A. Alterman, & P. Hunziker (Eds.), *Amino acid analysis: Methods and protocols*, (pp. 13–28). Humana Press.
- Schmidt-Nielsen, K., & Pennycuik, P. (1961). Capillary density in mammals in relation to body size and oxygen consumption. *American Journal of Physiology-Legacy Content*, **200**(4), 746–750.
- Schoors, S., De Bock, K., Cantelmo, A. R., Georgiadou, M., Ghesquière, B., Cauwenberghs, S., Kuchnio, A., Wong, B. W., Quaegebeur, A., Goveia, J., Bifari, F., Wang, X., Blanco, R., Tembuysen, B., Cornelissen, I., Bouché, A., Vinckier, S., Diaz-Moralli, S., Gerhardt, H., ... Carmeliet, P. (2014). Partial and transient reduction of glycolysis by PFKFB3 blockade reduces pathological angiogenesis. *Cell Metabolism*, **19**(1), 37–48.
- Scott, O., Vrbova, G., Hyde, S., & Dubowitz, V. (1985). Effects of chronic low frequency electrical stimulation on normal human tibialis anterior muscle. *Journal of Neurology, Neurosurgery & Psychiatry*, **48**(8), 774–781.
- She, P., Zhou, Y., Zhang, Z., Griffin, K., Gowda, K., & Lynch, C. J. (2010). Disruption of BCAA metabolism in mice impairs exercise metabolism and endurance. *Journal of Applied Physiology*, **108**(4), 941–949.
- Shimomura, Y., Murakami, T., Nakai, N., Nagasaki, M., & Harris, R. A. (2004). Exercise promotes BCAA catabolism: Effects of BCAA supplementation on skeletal muscle during exercise. *The Journal of Nutrition*, **134**(6), 1583S–1587S.
- Smith, J. A., Murach, K. A., Dyar, K. A., & Zierath, J. R. (2023). Exercise metabolism and adaptation in skeletal muscle. *Nature Reviews Molecular Cell Biology*, **24**(9), 607–632.
- Street, D., Bangsbo, J., & Juel, C. (2001). Interstitial pH in human skeletal muscle during and after dynamic graded exercise. *The Journal of Physiology*, **537**(3), 993–998.
- Takahashi, M., & Hood, D. A. (1993). Chronic stimulation-induced changes in mitochondria and performance in rat skeletal muscle. *Journal of Applied Physiology*, **74**(2), 934–941.
- Tickle, P. G., Hendrickse, P. W., Degens, H., & Egginton, S. (2020). Impaired skeletal muscle performance as a consequence of random functional capillary rarefaction can be restored with overload-dependent angiogenesis. *The Journal of Physiology*, **598**(6), 1187–1203.
- Walenta, S., Snyder, S., Haroon, Z. A., Braun, R. D., Amin, K., Brizel, D., Mueller-Klieser, W., Chance, B., & Dewhirst, M. W. (2001). Tissue gradients of energy metabolites mirror oxygen tension gradients in a rat mammary carcinoma model. *International Journal of Radiation Oncology* Biology* Physics*, **51**(3), 840–848.
- Walsby-Tickle, J., Gannon, J., Hvinden, I., Bardella, C., Abboud, M. I., Nazeer, A., Hauton, D., Pires, E., Cadoux-Hudson, T., Schofield, C. J., & McCullagh, J. S. O. (2020). Anion-exchange chromatography mass spectrometry provides extensive coverage of primary metabolic pathways revealing altered metabolism in IDH1 mutant cells. *Communications Biology*, **3**(1), 247.
- Warren, P. M., Kissane, R. W. P., Egginton, S., Kwok, J. C., & Askew, G. N. (2020). Oxygen transport kinetics underpin rapid and robust diaphragm recovery following chronic spinal cord injury. *The Journal of Physiology*.
- Williams, J. L., Weichert, A., Zakrzewicz, A., Da Silva-Azevedo, L., Pries, A. R., Baum, O., & Egginton, S. (2006). Differential gene and protein expression in abluminal sprouting and intraluminal splitting forms of angiogenesis. *Clinical Science*, **110**(5), 587–595.
- Williams, J. L., Cartland, D., Hussain, A., & Egginton, S. (2006). A differential role for nitric oxide in two forms of physiological angiogenesis in mouse. *The Journal of Physiology*, **570**(3), 445–454.
- Williams, J. L., Cartland, D., Rudge, J. S., & Egginton, S. (2006). VEGF trap abolishes shear stress-and overload-dependent angiogenesis in skeletal muscle. *Microcirculation*, **13**(6), 499–509.
- Williams, R., Walsby-Tickle, J., Hvinden, I. C., Legge, I., Kacerova, T., Lee, K. V., Misheva, M., Hauton, D., Ngere, J. B., & Sidda, J. D. (2025). Metabolomics using anion-exchange chromatography mass spectrometry for the analysis of cells, tissues and biofluids. *Nature Protocols*, **21**, 924–958.
- Xia, J., & Wishart, D. S. (2010). MSEA: A web-based tool to identify biologically meaningful patterns in quantitative metabolomic data. *Nucleic Acids Research*, **38**(Web Server), W71–W77.
- Young, S., & Egginton, S. (2009). Allometry of skeletal muscle fine structure allows maintenance of aerobic capacity during ontogenetic growth. *Journal of Experimental Biology*, **212**(21), 3564–3575.
- Zhang, B., Chen, Y., Shi, X., Zhou, M., Bao, L., Hatanpaa, K. J., Patel, T., DeBerardinis, R. J., Wang, Y., & Luo, W. (2021). Regulation of branched-chain amino acid metabolism by hypoxia-inducible factor in glioblastoma. *Cellular and Molecular Life Sciences*, **78**, 195–206.

Additional information

Data availability statement

Data are available via the University of Liverpool's Data Repository (<https://doi.org/10.17638/datacat.liverpool.ac.uk/3060>).

Competing interests

The authors declare that they have no competing interests.

Author contributions

R.W.P.K. and S.E. were responsible for the experimental design. R.W.P.K. and S.E. were responsible for animal surgery. R.W.P.K. was responsible for sample collection and histological analysis. D.H. and J.M. were responsible for metabolomics analysis. D.H. and R.W.P.K. were responsible for drafting the manuscript. All authors have read and approved the final version of this manuscript submitted for publication and agree to be accountable for all aspects of the work in ensuring that questions related to the accuracy or integrity of any part of the work are appropriately investigated and resolved. All persons designated as authors qualify for authorship, and all those who qualify for authorship are listed.

Funding

The School of Biomedical Sciences, University of Leeds provided a scholarship to RWPK.

Acknowledgements

We thank Dr John Walsby-Tickle, Department of Chemistry, University of Oxford, for technical support and the use of mass spectrometry facilities. We are grateful to the School of Biomedical Sciences, University of Leeds, for provision of a scholarship to RWPK.

Keywords

angiogenesis, exercise, hypoxia, metabolomics

Supporting information

Additional supporting information can be found online in the Supporting Information section at the end of the HTML view of the article. Supporting information files available:

Peer Review History